The earliest bird-line archosaurs and the assembly of the dinosaur body plan

Nesbitt, Sterling; Butler, Richard; Ezcurra, Martin; Barrett, Paul; Stocker, Michelle; Angielczyk, Kenneth; Smith, Roger; Sidor, Christian; Niedzwiedzki, Grzegorz; Sennikov, Andrey; Charig, Alan

DOI:
10.1038/nature22037

The earliest bird-line archosaurs and the assembly of the dinosaur body plan

Sterling J. Nesbitt[1*], Richard J. Butler[2], Martín D. Ezcurra[2,3], Paul M. Barrett[4], Michelle R. Stocker[1], Kenneth D. Angielczyk[5], Roger M.H. Smith[6,7] Christian A. Sidor[8], Grzegorz Niedźwiedzki[9], Andrey G. Sennikov[10,11], Alan J. Charig[†4]

[1]Department of Geosciences, Virginia Polytechnic Institute and State University, Blacksburg, VA, 24061, USA.
[2]School of Geography, Earth and Environmental Sciences, University of Birmingham, Edgbaston, Birmingham, B15 2TT, UK.
[3]CONICET−Sección Paleontología de Vertebrados, Museo Argentino de Ciencias Naturales, Buenos Aires, Argentina.
[4]Department of Earth Sciences, Natural History Museum, Cromwell Road, London, SW7 5BD, UK.
[5]Integrative Research Center, Field Museum of Natural History, 1400 South Lake Shore Drive, Chicago, IL 60605, USA.
[6]Evolutionary Studies Institute, University of the Witwatersrand, P.O. Wits 2050, Johannesburg, South Africa.
[7]Iziko South African Museum, P.O. Box 61, Cape Town, South Africa.
[8]Burke Museum and Department of Biology, University of Washington, Seattle, WA 98195, USA.
[9]Department of Organismal Biology, Uppsala University, Norbyvägen 18A, 752 36 Uppsala, Sweden.
[10]Borissiak Paleontological Institute, Russian Academy of Sciences, Profsoyuznaya 123, Moscow 117997, Russia.
[11]Kazan Federal University, Kremlyovskaya ul. 18, Kazan, 420008 Russia.
[†]Deceased

The relationship of dinosaurs to other reptiles is well-established[1-4], but the sequence of acquisition of dinosaurian features has been obscured by the scarcity of fossils recording transitional morphologies. The closest extinct relatives of dinosaurs have either highly-derived morphologies[5-7], or are known from poorly preserved[8,9] or incomplete material[10,11]. Here, we report one of the stratigraphically lowest and phylogenetically earliest members of the avian stem lineage (Avemetatarsalia), *Teleocrater rhadinus* gen. et sp. nov., from the Middle Triassic. The anatomy of *T. rhadinus* provides key information that unites several enigmatic taxa from across

Pangaea into a previously unrecognized clade, Aphanosauria. This clade is the sister taxon of Ornithodira (pterosaurs + birds) and shortens the ghost lineage inferred at the base of Avemetatarsalia. We demonstrate that several anatomical features long thought to characterise Dinosauria and dinosauriforms evolved much earlier, soon after the bird-crocodylian split, and that the earliest avemetatarsalians retained the crocodylian-like ankle morphology and hind limb proportions of stem archosaurs and early pseudosuchians. Early avemetatarsalians were significantly more species-rich, widely geographically distributed, and morphologically diverse than previously recognized. Moreover, several early dinosauromorphs that were previously used as models to understand dinosaur origins may represent specialised forms rather than the ancestral avemetatarsalian morphology.

Birds and crocodylians– which are each other's closest living relatives and form the clade Archosauria– diverged in the Triassic[2,3]. The divergence of stem-avians (Avemetatarsalia) from stem-crocodylians (Pseudosuchia) is a major transition in terrestrial vertebrate evolution, involving changes in limb proportions and body size, numerous morphological innovations in the hind limb, and, eventually, extensive forelimb modification in dinosaurs[2,12-14]. However, those changes are poorly documented because of a limited fossil record, especially for the Middle Triassic. For example, the earliest diverging group of currently known stem-avians, the pterosaurs, were already highly specialised by the time of their first appearance in the Late Triassic, providing few clues about sequences of character evolution in early stem-avians. Other key early diverging stem-avian taxa are known only from limited postcranial remains (e.g.

lagerpetids[10,15]). Thus, a clear morphological gap currently exists between dinosaurs, pterosaurs, and stem-crocodylians.

Here, we name and describe the oldest member of the avian stem lineage from the lower strata of the Middle Triassic Manda Beds of Tanzania (Fig. 1). This taxon substantially enhances our knowledge of the origin and early evolution of the stem-avian anatomical features that are characteristic of dinosaurs, while also revealing a previously undocumented combination of morphologies retained from the common ancestor of birds and crocodylians.

Archosauria Cope, 1869 *sensu* Gauthier and Padian, 1985

Avemetatarsalia Benton, 1999

Aphanosauria clade nov. (see methods)

Teleocrater rhadinus gen. et sp. nov.

Etymology. 'Teleos', finished or complete (Greek) and 'krater', bowl or basin (Greek), referring to the closed acetabulum; 'rhadinos', slender (Greek), referring to the slender body plan.

Holotype. NHMUK PV R6795, a disassociated skeleton of one individual, including: cervical, trunk, and caudal vertebrae, partial pectoral and pelvic girdles, partial forelimb and hind limbs (Fig. 2a, d, g-k, m, o; Supplementary Information Table S1 and S2).

Referred Material. Elements found near the holotype, but from other individuals, which

represent most of the skeleton and that are derived from a paucispecific bonebed containing at least three individuals (Fig. 2; Supplementary Information Table S3).

Locality and horizon. Near the base of the Lifua Member of the Manda Beds (Anisian based on biostratigraphical correlations with the *Cynognathus* Subzone B Assemblage Zone of South Africa[16]), Ruhuhu Basin, Tanzania[17]; stratigraphically below the formerly oldest stem-avian *Asilisaurus kongwe*[7] and other members of the typical faunal assemblage from the Manda Beds[18] (Fig. 1).

Diagnosis. *Teleocrater rhadinus* differs from all other archosauriforms in the following combination of character states (*=probable autapomorphy): neural canal openings of the anterior cervicals dorsoventrally elongated anteriorly and mediolaterally elongated posteriorly*; anterior cervicals at least 1.5 times longer than anterior to middle trunk vertebrae; preacetabular process of the ilium arcs medially to create a distinct pocket on the medial surface; small concave ventral margin of the ischial peduncle of the ilium; long iliofibularis crest of the fibula (see Supplementary Information for differential diagnosis).

Description. The maxilla bears a prominent antorbital fossa that extends onto the posterior process and a medially extended palatal process that likely contacted its counterpart, both apomorphic conditions of Archosauria[19]. The single preserved tooth crown is labiolingually compressed, recurved and finely serrated on both margins. The frontal possesses a shallow, but prominent, supratemporal fossa, as in all early

dinosaurs[13,14].

As in dinosauriforms, the anterior cervical vertebrae are significantly longer than the axis and the posterior cervical vertebrae; proportionally, they are among the longest of any Triassic avemetatarsalians (up to ~3.5 times longer than high). The anterior and middle cervical vertebrae possess posteriorly projecting epipophyses. The posterior cervical vertebrae have an extra articular surface between the parapophysis and diapophysis for three-headed ribs, similar to early crocopods, *Yarasuchus*, and some pseudosuchians[19,20]. The elongated trunk vertebrae have well developed hyposphene-hypantrum articulations. *Teleocrater* possesses two sacral vertebrae, compared to three in *Nyasasaurus*[21]. The sacral rib of the second sacral vertebra bears posterolaterally directed processes, which are known only in *Yarasuchus*, *Spondylosoma*, and dinosauriforms among archosaurs (Supplementary Information). Osteoderms are not preserved and were likely absent.

The scapula has a distinct acromion process, as in most archosaurs and their close relatives (e.g. proterochampsids[20]). The posterior scapular margin bears a thin proximodistally-oriented ridge, which is also present in silesaurids (Supplementary Information), and the glenoid fossa of the scapula is oriented mostly posteroventrally. The deltopectoral crest of the humerus is >30% the length of the element, similar to *Nyasasaurus*[21] and dinosaurs[22], but unlike silesaurids and pterosaurs. From a single recovered metacarpal we infer that the hand was small relative to the rest of the forelimb.

The acetabulum of *Teleocrater* was closed, but a small concave notch on the ischial peduncle suggests a small perforation of the acetabulum, as in *Asilisaurus*[7] and *Silesaurus*[6]. A distinct vertical crest extending dorsally from the supraacetabular rim

separates a medially projecting preacetabular process from the rest of the ilium, similar to *Marasuchus*[11] and *Asilisaurus*[7].

The proximal surface of the femur of *Teleocrater* has a deep longitudinal groove, and there is no anteromedial tuber (= posteromedial tuber[20]), unlike nearly all archosaurs[19,20]. As in dinosauromorphs, a proximally placed M. iliofemoralis externus scar is present and connected to the anterior intermuscular line. However, in *Teleocrater* the M. iliofemoralis externus scar is well separated from the M. iliotrochantericus caudalis scar and lies in the plesiomorphic position present in early archosaurs and their close relatives[19], as well as in *Dongusuchus* and *Yarasuchus* (Extended Data Fig. 1). The posterior surface of the distal medial condyle possesses a proximodistally-oriented scar that is also present in dinosauromorphs (Supplementary Information). The tibia lacks a cnemial crest and any differentiation of its distal end, contrasting with proterochampsids and dinosauromorphs[19,20]. The proximal half of the fibula has a long, twisted iliofibularis crest. The calcaneum bears the character states of a 'crocodile-normal' ankle configuration, a concave astragalar facet that permitted movement between the calcaneum and astragalus, as well as a taller than broad and posteriorly directed calcaneal tuber and a distinctly rounded fibular facet. Osteohistology of the *Teleocrater* humerus and fibula suggest sustained, elevated growth rates (Extended Data Fig. 2; Supplementary Information) similar to those of many ornithodirans[21,23].

Our phylogenetic analyses recovered *Teleocrater* in a clade containing *Yarasuchus*, *Dongusuchus*, and *Spondylosoma*. This previously unrecognised clade, named Aphanosauria herein, is resolved as the earliest diverging group on the avian stem lineage (Extended Data Figs. 3 and 4; Supplementary Information). The body plans of

Teleocrater and other aphanosaurs demonstrate a previously undocumented transitional morphology between the common ancestor of archosaurs and dinosaurs and their closest relatives. Aphanosaurs were long-necked, non-cursorial, and carnivorous, and so more like stem-archosaurs and pseudosuchians than later avemetatarsalians. *Teleocrater* confirms that several key character states of the ankle that together form the 'crocodile-normal' configuration are plesiomorphic for both Archosauria and Avemetatarsalia. The distribution of ankle morphologies among early dinosauriforms is much more complex than previously appreciated, with 'crocodile-normal' character states retained by the silesaurids *Lewisuchus* and *Asilisaurus*[7], *Marasuchus*, and some early dinosaurs (Extended Data Fig. 5). This implies repeated evolution within Avemetatarsalia of the character states typical of the 'advanced mesotarsal' ankle configuration present in pterosaurs, lagerpetids, and dinosaurs, although the functional implications of these convergent acquisitions require rigorous biomechanical evaluation (see Supplemental Information).

Several of the character states supporting Aphanosauria at the base of Avemetatarsalia were once thought to characterise only dinosaurs (e.g. supratemporal fossa on the frontal[2]) or dinosauriforms (e.g. hyposphene-hypantra in trunk vertebrae[2]), but *Teleocrater* demonstrates that these morphologies have a deeper history. Comparison of the hind limb proportions (femur-tibia-longest metatarsal ratios) of early archosaurs and close relatives indicates that *Teleocrater* and silesaurids have proportions similar to those of stem-archosaurs and pseudosuchians (Extended Data Fig. 6), and that these proportions probably represent the ancestral avemetatarsalian condition. Lagerpetids, pterosaurs, and small- to medium-sized dinosaurs (e.g. early ornithischians,

coelophysoids) all lengthened the metatarsus relative to the femur and tibia, in association with increasingly cursorial adaptations[26]. However, it is currently unclear how many times these hind limb modifications evolved independently given the complex distribution of character states among these taxa.

Aphanosaurs, like the earliest pseudosuchians[27,28], were widespread across Pangaea during the Middle Triassic, and the major subclades of avemetatarsalians (e.g. Aphanosauria, Lagerpetidae, Silesauridae, Dinosauria) underwent repeated biogeographic expansions across Pangaea throughout the Middle and Late Triassic (Fig. 3). The discoveries of Aphanosauria and other specialized Triassic avemetatarsalians call into question the hypothesis that pseudosuchians were more morphologically disparate than avemetatarsalians during the Triassic[29,30]. We estimated weighted mean pairwise disparity for Avemetatarsalia and Pseudosuchia using a data matrix including the new information presented here and, in contrast with previous analyses[29,30], found no significant difference in disparity between the clades for the entire dataset or for any individual time bin (Fig. 3).

Aphanosaurs, and other discoveries, demonstrate that early avemetatarsalians had much more complex biogeographic and evolutionary histories than previously appreciated. Analyses of dinosaur origins have usually assumed that their immediate ancestors resembled highly cursorial taxa such as *Marasuchus* and *Lagerpeton*. This assumption is challenged by the recognition of non-cursorial avemetatarsalian taxa such as aphanosaurs and silesaurids, indicating that current models of dinosaur origins are in need of revision.

Supplementary Information is linked to the online version of the paper at http://www.nature.com/nature.

Acknowledgements We acknowledge A. Tibaijuka for help with fieldwork logistics in Tanzania. Supported by National Geographic Society Research & Exploration grant (#9606-14, SJN), National Science Foundation EAR-1337569 (CAS) and EAR-1337291 (KDA, SJN), a Marie Curie Career Integration Grant (630123, RJB), a National Geographic Society Young Explorers grant (9467-14 MDE), and the Russian Government Program of Competitive Growth of Kazan Federal University and RFBR 14-04-00185, 17-04-00410 (AGS). We thank S. Chapman, A. C. Milner, M. Lowe, and S. Bandyopadhyay for access to specimens, S. Werning, G. Lloyd, R. Close, and K. Padian for discussions, and H. Taylor provided photographs of the holotype.

Author Contributions Nesbitt, Butler, Ezcurra, and Barrett designed the research project; Sidor and Angielczyk designed the field project; Nesbitt, Sidor, Angielczyk, Smith, and Stocker conducted fieldwork; Nesbitt, Butler, Ezcurra, Barrett, Stocker, and Charig described the material; Nesbitt, Ezcurra, and Stocker conducted the phylogenetic analyses; Butler conducted disparity analyses; and Nesbitt, Butler, Ezcurra, Barrett, Stocker, Angielczyk, Smith, Sidor, Niedźwiedzki, and Sennikov wrote the manuscript.

Author Information Reprints and permissions information is available at www.nature.com/reprints. The authors declare no competing financial interests. Correspondence and requests for materials should be addressed to S.J.N.

(sjn2104@vt.edu).

REFERENCES

1 Benton, M. J. & Clark, J. M. in *The Phylogeny and Classification of the Tetrapods, Volume 1: Amphibians, Reptiles, Birds Systematics Association Special Volume 35A* (ed M. J. Benton) 295-338 (Clarendon Press, 1988).

2 Gauthier, J. Saurischian monophyly and the origin of birds. *Memoirs of the California Academy of Sciences* **8**, 1-55 (1986).

3 Sereno, P. C. Basal archosaurs: phylogenetic relationships and functional implications. *Society of Vertebrate Paleontology Memoir* **2**, 1-53 (1991).

4 Sereno, P. C. The evolution of dinosaurs. *Science* **284**, 2137-2147 (1999).

5 Dalla Vecchia, F. M. in *Anatomy, Phylogeny, and Palaeobiology of Early Archosaurs and their Kin* Vol. 379 (eds S.J. Nesbitt, J.B. Desojo, & R.B. Irmis) 119-155 (Geological Society, London, Special Volume, 2013).

6 Dzik, J. A beaked herbivorous archosaur with dinosaur affinities from the early Late Triassic of Poland. *Journal of Vertebrate Paleontology* **23**, 556-574 (2003).

7 Nesbitt, S. J. *et al.* Ecologically distinct dinosaurian sister group shows early diversification of Ornithodira. *Nature* **464**, 95-98 (2010).

8 Benton, M. J. *Scleromochlus taylori* and the origin of dinosaurs and pterosaurs. *Philosophical Transactions of the Royal Society of London, Series B* **354**, 1423-1446 (1999).

9 Benton, M. J. & Walker, A. D. *Saltopus*, a dinosauriform from the Upper Triassic of Scotland. *Earth and Environmental Science Transactions of the Royal Society*

of Edinburgh **101**, 285-299 (2011).

10 Sereno, P. C. & Arcucci, A. B. Dinosaurian precursors from the Middle Triassic of Argentina: *Lagerpeton chanarensis*. *Journal of Vertebrate Paleontology* **13**, 385-399 (1994).

11 Sereno, P. C. & Arcucci, A. B. Dinosaurian precursors from the Middle Triassic of Argentina: *Marasuchus lilloensis*, gen. nov. *Journal of Vertebrate Paleontology* **14**, 53-73 (1994).

12 Bakker, R. T. & Galton, P. M. Dinosaur monophyly and a new class of vertebrates. *Nature* **248**, 168-172 (1974).

13 Brusatte, S. L. *et al.* The origin and early radiation of dinosaurs. *Earth-Science Reviews* **101**, 68-100 (2010).

14 Langer, M. C., Ezcurra, M. D., Bittencourt, J. S. & Novas, F. E. The origin and early evolution of dinosaurs. *Biological Reviews* **85**, 55-110 (2010).

15 Irmis, R. B. *et al.* A Late Triassic dinosauromorph assemblage from New Mexico and the rise of dinosaurs. *Science* **317**, 358-361 (2007).

16 Rubidge, B. S. Re-uniting lost continents - fossil reptiles from the ancient Karoo and their wanderlust. *South African Journal of Geology* **108**, 135-172 (2005).

17 Wopfner, H. Tectonic and climatic events controlling deposition in Tanzanian Karoo basins. *Journal of African Earth Sciences* **34**, 167-177 (2002).

18 Sidor, C. A. *et al.* Provincialization of terrestrial faunas following the end-Permian mass extinction. *Proceedings of the National Academy of Sciences* **110**, 8129-8133, doi: 10.1073/pnas.1302323110 (2013).

19 Nesbitt, S. J. The early evolution of archosaurs: relationships and the origin of

major clades. *Bulletin of the American Museum of Natural History* **352**, 1-292 (2011).

20 Ezcurra, M. D. The phylogenetic relationships of basal archosauromorphs, with an emphasis on the systematics of proterosuchian archosauriforms. *PeerJ* **4**, e1778; DOI 1710.7717/peerj.1778 (2016).

21 Nesbitt, S. J., Barrett, P. M., Werning, S., Sidor, C. A. & Charig, A. The oldest dinosaur? A Middle Triassic dinosauriform from Tanzania. *Biology Letters* **9**, doi:10.1098/rsbl.2012.0949 (2013).

22 Langer, M. C. & Benton, M. J. Early dinosaurs: A phylogenetic study. *Journal of Systematic Palaeontology* **4**, 309-358 (2006).

23 Padian, K., Horner, J. R. & de Ricqlès, A. Growth in small dinosaurs and pterosaurs: the evolution of archosaurian growth strategies. *Journal of Vertebrate Paleontology* **24**, 555-571 (2004).

24 Chatterjee, S. Phylogeny and classification of thecodontian reptiles. *Nature* **295**, 317-320 (1982).

25 Cruickshank, A. & Benton, M. Archosaur ankles and the relationships of the thecodontian and dinosaurian reptiles. *Nature* **317**, 715-717 (1985).

26 Kubo, T. & Kubo, M. O. Associated evolution of bipedality and cursoriality among Triassic archosaurs: a phylogenetically controlled evaluation. *Paleobiology* **38**, 474-485 (2012).

27 Butler, R. J. *et al.* The sail-backed reptile *Ctenosauriscus* from the latest Early Triassic of Germany and the timing and biogeography of the early archosaur radiation. *PLoS One* **6**, e25693, 25691-25628 (2011).

28 Butler, R. J. *et al.* New clade of enigmatic early archosaurs yields insights into early pseudosuchian phylogeny and the biogeography of the archosaur radiation. *BMC Evolutionary Biology* **14**, 128 (2014).

29 Brusatte, S. L., Benton, M. J., Lloyd, G. T., Ruta, M. & Wang, S. C. Macroevolutionary patterns in the evolutionary radiation of archosaurs (Tetrapoda: Diapsida). *Earth and Environmental Science Transactions of the Royal Society of Edinburgh* **101**, 367-382 (2011).

30 Brusatte, S. L., Benton, M. J., Ruta, M. & Lloyd, G. T. Superiority, competition, and opportunism in the evolutionary radiation of dinosaurs. *Science* **321**, 1485-1488 (2008).

FIGURES

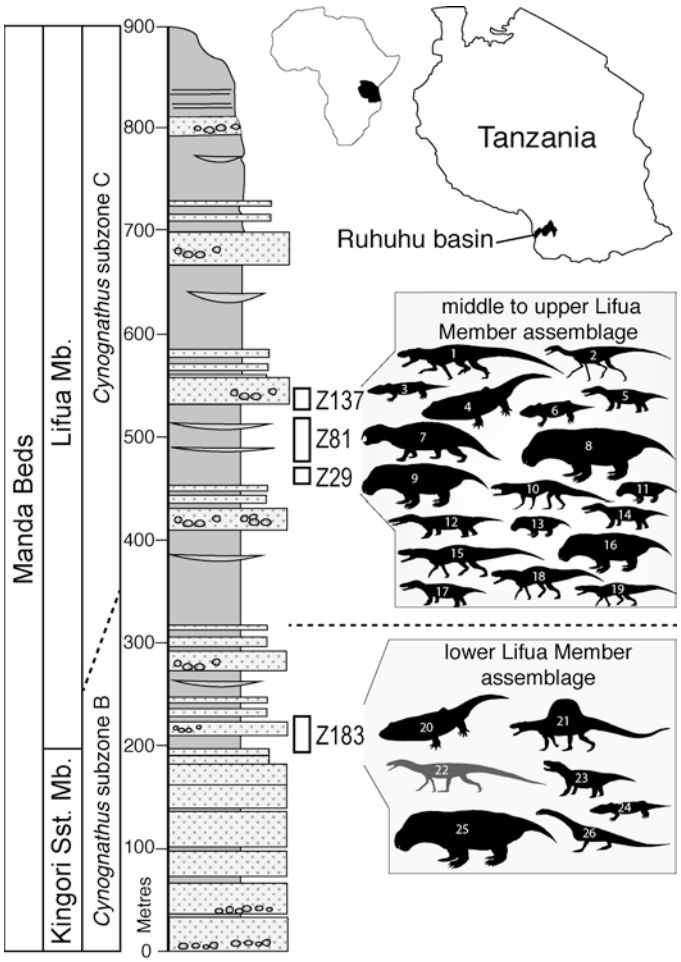

Figure 1 | Geographical and stratigraphical occurrence of *Teleocrater rhadinus* gen. et sp. nov. from the Ruhuhu Basin, southern Tanzania, Africa. Numbered silhouettes refer to taxa with voucher specimens in Supplementary Information S4. *Nyasasaurus parringtoni* is not included because its stratigraphic position is not clear. See Methods for silhouette sources. Z numbers refers to localities. Mb., member; Sst., sandstone. [one column]

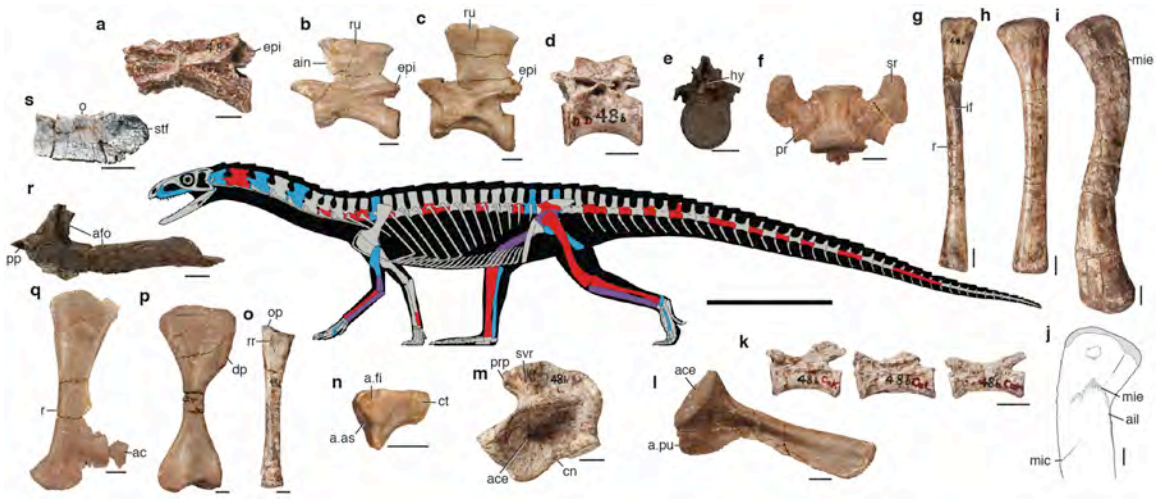

Figure 2 | Skeletal anatomy of *Teleocrater rhadinus* gen et sp. nov. a–c, Anterior and mid cervical vertebrae (NHMUK PV R6795, NMT RB505, NMT RB511). **d–e**, Middle and posterior trunk vertebrae (NHMUK PV R6795). **f**, Second sacral vertebra (NMT RB519). **g**, Left fibula (NHMUK PV R6795). **h**, Right tibia (NHMUK PV R6795). **i**, Left femur (NHMUK PV R6795). **j**, Muscle scars of right femur (NHMUK PV R6795). **k**, Posterior caudal vertebrae (NHMUK PV R6795). **l**, Left ischium (NMT RB479). **m**, Partial left ilium (NHMUK PV R6795). **n**, Right calcaneum (NMT RB490). **o**, Left ulna (NHMUK PV R6795). **p**, Left humerus (NMT RB476). **q**, Right scapula (NMT RB480). **r**, Left maxilla (NMT RB495). **s**, Right frontal (NMT RB496). Orientations: **a–d**, **k**, left lateral; **e**, posterior; **f**, ventral; **g**, **h**, **l**, **m**, **o**, **q**, **r**, lateral; **i**, **j**, anterolateral; **n**, proximal; **p**, anterior; **s**, dorsal. Scales: **a**–**s**, 1 cm; skeleton, 25 cm. Red = holotype, blue = referred, purple = in holotype and referred, gray = unknown. a., articulates with; ac, acromion; ace, acetabulum; afo, antorbital fossa; ain, anteriorly inclined anterior margin of the neural spine; as, astragalus; cn, concave notch; ct, calcaneal tuber; dp, deltopectoral crest; epi, epipophyses; fi, fibula; hy, hyposphene; if, M. iliofemoralis scar; lic, linea intermuscularis cranialis; mic, M. iliotrochantericus caudalis scar; mie, M. iliofemoralis

externus scar; NHMUK, Natural History Museum, London, U.K.; NMT, National Museum of Tanzania, Dar es Salaam, Tanzania, o, orbital margin; op, olecranon process; pp, palatal process; pr, posterolateral process; prp, preacetabular process; pu, pubis; r, ridge; rr, radius ridge; ru, rugosity; sr, sacral rib; stf, supratemporal fossa; svr, subvertical ridge. [two columns]

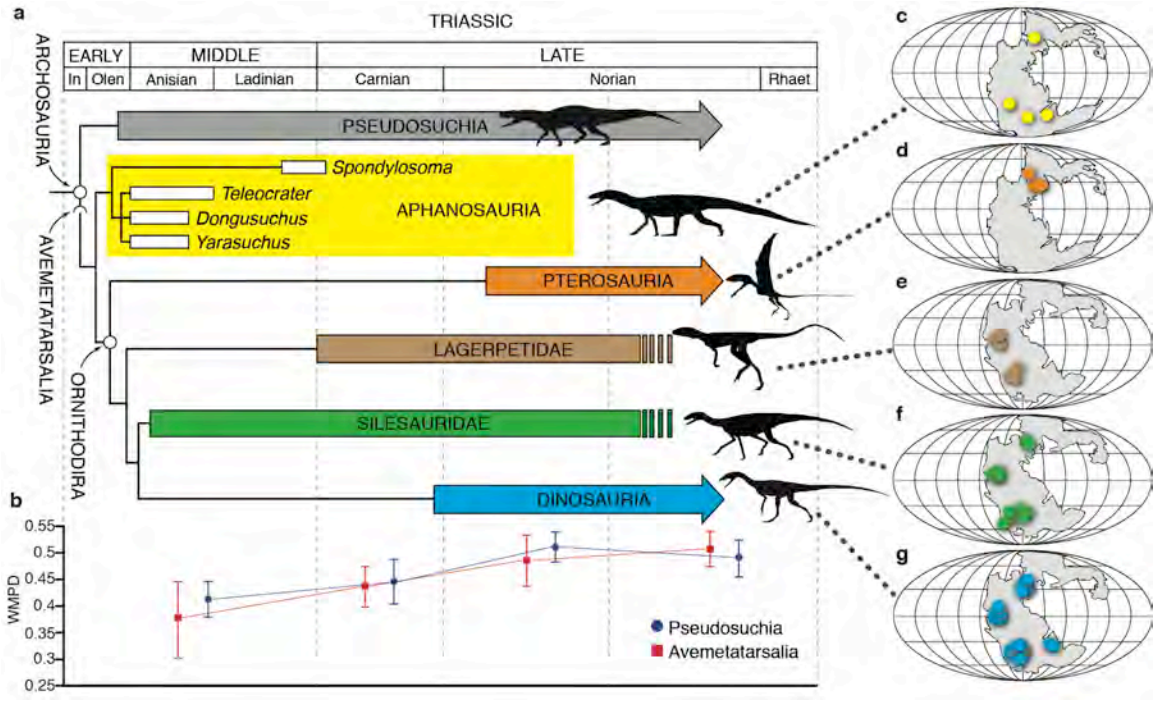

Figure 3 | Early evolution of avemetatarsalians. a, Interrelationships of Avemetatarsalia derived from two datasets[19,20] (Supplementary Information). All clades except Aphanosauria have been collapsed for clarity. The lengths of the white bars indicate stratigraphic imprecision. **b**, Plot of morphological disparity for Pseudosuchia (including Phytosauria) and Avemetatarsalia for the duration of the Triassic. Plots show weighted mean pairwise dissimilarity (see methods). **c**-**g**, Geographical distributions of major subclades of avemetatarsalians during the Triassic. **c**, Aphanosauria. **d**, Pterosauria. **e**, Lagerpetidae. **f**, Silesauridae. **g**, Dinosauria. See Supplementary Table S5 for

occurrences. In, Induan; Olen, Olenekian; Rhaet, Rhaetian. Palaeogeographic maps modified from https://www2.nau.edu/rcb7/globaltext2.html. [two columns]

Methods

Systematic Paleontology.

Aphanosauria clade nov.

Etymology. ‘Aphanes’, hidden or obscure (Greek) and ‘sauros’, for lizard (Greek).

Definition. The most inclusive clade containing *Teleocrater rhadinus* and *Yarasuchus deccanensis* Sen, 2005 but not *Passer domesticus* Linnaeus, 1758 or *Crocodylus niloticus* Laurenti, 1768.

Diagnosis. Aphanosauria differs from all other archosaurs in possessing the following unique combination of character states: elongate cervical vertebrae with epipophyses and anteriorly overhanging neural spines that have rugose lateral margins on their dorsal ends; elongated deltopectoral crest that is at least 35% the length of the humerus; wide distal end of the humerus; femur with a scar for the M. iliofemoralis externus near the proximal surface (homologous with the anterior trochanter in dinosauromorphs) that is separate from the scar for the M. iliotrochantericus caudalis (homologous with the trochanteric shelf in dinosauromorphs), without an anteromedial tuber, and with a straight, deep groove in the proximal surface; calcaneal tuber taller than broad (see Supplementary Information).

Histology. We sampled two specimens, a partial right fibula consisting of the proximal and distal ends (NMT RB488; Extended Data Fig. 1) and a left humerus (NMT RB476; Extended Data Fig. 2). We sampled close to the midshaft for NMT RB488 by extracting

a small piece located at the proximal-most preserved portion of the distal end; a small chip was removed from the midshaft of NMT RB476 (Extended Data Fig. 2). Taking advantage of natural cracks in both specimens, the target portions of the bones were removed by applying acetone to the surface followed by gentle pressure to remove the pieces. The pieces were embedded in a clear polyester resin (Castolite AP) under vacuum. The block of polyester resin was cut into 1 mm thick thin-sections using an Isomet 1000 saw (Buehler Inc., Lake Bluff, IL, USA) equipped with a diamond wafering blade. The thin-sections were adhered to plastic slides using Aron Alpha (Type 201) cyanoacrylate. Both sections were then ground down using standard practices[31] to the point at which light could pass through the bone. The thin-sections were imaged with regular transmitted light (brightfield) and a full wave retarder (lambda = 530 nm) (Extended Data Fig. 2).

Phylogenetic analysis. The relationships of *Teleocrater rhadinus* were analyzed using the two most comprehensive, and largely independent, datasets available for Triassic archosauromorphs[19,20]. Both matrices were analyzed under equally weighted parsimony using TNT 1.5[32,33]. A heuristic search with 100 replicates of Wagner trees (with a random addition sequence) followed by TBR branch-swapping (holding 10 trees per replicate) was performed. The best trees obtained from the replicates were subjected to a final round of TBR branch swapping. Zero-length branches in any of the recovered MPTs were collapsed. Decay indices (=Bremer support values) were calculated and a bootstrap resampling analysis, using 1,000 pseudoreplicates, was performed reporting both absolute and GC (i.e. difference between the frequencies of recovery in pseudoreplicates of the original group and the most frequently recovered contradictory group) frequencies.

We added and deleted various taxa from the Nesbitt analysis[19], based on more recent publications. We included new data (*Yonghesuchus sangbiensis* and character 413)[28] and excluded the wildcard taxa *Parringtonia gracilis* and *Erpetosuchus granti*[28]. We added the holotype and referred femora of *Dongusuchus efremovi*, the hypodigm of *Yarasuchus deccanensis* (see Supplementary Information), and *Spondylosoma absconditum* (see Supplementary Information) for a total of 82 taxa. We did not include non-femoral elements from *Dongusuchus efremovi* because of uncertainty of association and attribution to the taxon[34]. We employed a conservative scoring strategy for those newly added taxa that are represented by more than one specimen. We scored the holotype of *Teleocrater rhadinus* and all the referred material of the same taxon separately, and then combined them into a '*Teleocrater* combined' terminal taxon. Similarly, we added information from a nearly complete, single skeleton of *Asilisaurus kongwe* (NMT RB159) under the terminal taxon name '*Asilisaurus kongwe* skeleton' and then combined those scores with the original holotype and referred material of *Asilisaurus kongwe*[7]. Additionally, we scored the enigmatic taxon *Scleromochlus taylori* into the phylogeny (Extended Data Figs. 7, 8; see Supplementary Information). For the Ezcurra dataset[20], we used the taxon sampling of his analysis 3[20],with the addition of *Spondylosoma absconditum*, *Scleromochlus taylori*, and *Teleocrater rhadinus*. For the latter two taxa we used the same strategy as for the Nesbitt dataset[19], and this resulted in a total of 86 taxa.

A few characters were modified and six new characters (414−419; see Supplemental Information) were added to the Nesbitt dataset[19] for a total of 419 characters. The following characters were ordered in this dataset: 32, 52, 121, 137, 139,

156, 168, 188, 223, 247, 258, 269, 271, 291, 297, 328, 356, 399, and 413. Five of the six new characters (601−605) added to the Nesbitt matrix were included in the Ezcurra dataset. The remaining character was not added because it was already included in the original version of this matrix. Fusion between the astragalus and calcaneum was added as an independent character (606) rather than as a state of character 532. Taxa with a fused astragalocalcaneum (e.g. *Lagerpeton chanarensis*) were re-scored as inapplicable for character 532. The modified data matrix contains a total of 606 characters. The following characters were ordered in the Ezcurra dataset[20]: 1, 2, 7, 10, 17, 19, 20, 21, 28, 29, 36, 40, 42, 50, 54, 66, 71, 75, 76, 122, 127, 146, 153, 156, 157, 171, 176, 177, 187, 202, 221, 227, 263, 266, 279, 283, 324, 327, 331, 337, 345, 351, 352, 354, 361, 365, 370, 377, 379, 398, 410, 424, 430, 435, 446, 448, 454, 458, 460, 463, 472, 478, 482, 483, 489, 490, 504, 510, 516, 529, 537, 546, 552, 556, 557, 567, 569, 571, 574, 581, 582, and 588.

Disparity analysis. We estimated morphological disparity using the modified Nesbitt data matrix (Fig. 3; Supplementary Information Fig. S5). We chose this data matrix because its taxonomic and anatomical sampling of Triassic crown archosaurs is the most comprehensive available (whereas the Ezcurra data matrix focuses primarily on stem-archosaurs). We supplemented this dataset by scoring a number of additional pseudosuchian and avemetatarsalian species, resulting in a final taxon list of 114 operational taxonomic units. From these data we estimated disparity for four time bins covering the Triassic archosaur radiation: (1) late Early Triassic–Middle Triassic; (2) Carnian; (3) early Norian; (4) late Norian–Rhaetian.

Disparity was estimated for three different groupings: (1) Avemetatarsalia; (2) Pseudosuchia without Phytosauria; (3) Pseudosuchia with Phytosauria (Figure 3;

Extended Data Fig. 9). The latter grouping was chosen to reflect the traditional inclusion of Phytosauria within Pseudosuchia (as also recovered in the second of our phylogenetic analyses, based on the Ezcurra data matrix). Outgroup taxa were excluded from the data matrix prior to analysis. All ingroup taxa were assigned to one of the time bins. Nevertheless, *Machaeroprosopus pristinus* was assigned to both early Norian and late Norian–Rhaetian time bins, in order to ensure that phytosaur morphology was included in disparity calculations for all time bins in which the group is known to have been present.

Disparity was calculated as weighted mean pairwise dissimilarity (WMPD)[35,36] in the R package Claddis[36]. Results are presented in Supplementary Information Table S6. Bootstrapped 95% confidence intervals were calculated for WMPD using 1000 replicates. Disparity was calculated for each group in each time bin, as well as total disparity for each group, including all of its Triassic representatives.

Hind limb disparity. In order to examine changes in hind limb proportions among archosauriforms, we collected data on the lengths of the femur, tibia, and metatarsals III and IV, as well as the proximal widths of these two metatarsals, for 96 individuals representing 49 species, including four species of non-archosaurian archosauriforms, 17 pseudosuchian species, eight pterosaur species, 13 dinosaur species, and seven species of non-dinosaurian, non-pterosaurian avemetatarsalians (including aphanosaurs, silesaurids, lagerpetids, and *Marasuchus*) (Supplementary Information Table S7). Data were collected from the literature and directly from specimens.

For *Teleocrater rhadinus*, complete lengths of metatarsals III and IV were not available, although the proximal ends of both are preserved. In order to estimate the complete length of metatarsal III we conducted an ordinary least squares linear

regression, using the proximal width of metatarsal III as the independent variable and metatarsal III length as the dependent variable (Supplementary Information Table S8). Data were $\log_{10}$-transformed prior to analysis. The formula of the resultant regression model (y = 0.634x + 1.09357; R^2 = 0.68, p = 1.285e-08) was used to estimate a length of 74.8 mm for metatarsal III of *Teleocrater rhadinus*. In order to visualize the hindlimb proportions for taxa in our dataset, we plotted them onto a ternary diagram using the R package ggtern[37] (Extended Data Fig. 6; Supplementary Information). Different symbols were used to plot the five major groups of archosauriforms covered by our data (see above), and the fill of the symbols was coloured according to femur length. Statistical analyses and plotting of data were conducted in R[38].

All data (e.g., R scripts, measurements used for the disparity analysis, phylogenetic datasets) that support the findings of this study are available at Dryad with the identifier [XXXXXXX].

Further sources for silhouettes and reconstructions in Figures 1–3. In figure 1, taxa 1, 15, 18, 19, and 21 from[19]. 2 by Scott Hartman. 3, 4, 6, 20, and 24 (Public Domain Dedication 1.0) from Phylopic.org. 7 by Steven Traver (Public Domain Dedication 1.0) from Phylopic.org. The skeletal reconstruction in figure 2 and the silhouettes of the pterosaur, silesaurid, and dinosaur in figure 3 are by Scott Hartman.

31 Lamm, E.-T. in *Bone histology of fossil tetrapods: Advancing methods, analysis, and interpretation* (eds K. Padian & E.-T. Lamm) 55-160 (University of

California Press, 2013).

32 Goloboff, P., Farris, J. & Nixon, K. TNT: a free program for phylogenetic analysis. *Cladistics* **24**, 774-786 (2008).

33 Goloboff, P. A. & Catalano, S. A. TNT version 1.5, including a full implementation of phylogenetic morphometrics. *Cladistics* **32**, 221-238 (2016).

34 Niedźwiedzki, G., Sennikov, A. & Brusatte, S. L. The osteology and systematic position of *Dongusuchus efremovi* Sennikov, 1988 from the Anisian (Middle Triassic) of Russia. *Historical Biology* **28**, 550-570, DOI: 510.1080/08912963.08912014.08992017 (2016).

35 Close, R. A., Friedman, M., Lloyd, G. T. & Benson, R. B. Evidence for a mid-Jurassic adaptive radiation in mammals. *Current Biology* **25**, 2137-2142 (2015).

36 Lloyd, G. T. Estimating morphological diversity and tempo with discrete character-taxon matrices: implementation, challenges, progress, and future directions. *Biological Journal of the Linnean Society* (2016).

37 ggtern: An extension to 'ggplot2', for the creation of ternary diagrams. R package version 2.1.5. https://CRAN.R-project.org/package=ggtern (2016).

38 R: A language and environment for statistical computing. (R Foundation for Statistical Computing, Vienna, Austria, 2013).

Extended Data Figure 1. Skeletal anatomy of the aphanosaurs *Dongusuchus efremovi* (a-b), *Yarasuchus deccanensis* (c-t), and *Spondylosoma absconditum* (u-cc). Left holotype femur of *Dongusuchus* (PIN 952/15-1) in **a,** posteromedial and **b,**

anterolateral views. Right partial femur of *Yarasuchus* (ISIR unnumbered) in **c**, posterolateral **d**, proximal, and **e**, anterolateral views. Left tibia of *Yarasuchus* (ISIR 334) in **f**, posterior and **g**, distal views. Left calcaneum of *Yarasuchus* (ISIR unnumbered) in **h**, proximal and **i**, lateral views. **j**, Second sacral vertebra of *Yarasuchus* (ISIR BIA 45/43) in ventral view. **k**, Right ischium of *Yarasuchus* (ISIR 334) in ventrolateral view. Posterior cervical vertebrae of *Yarasuchus* (ISIR BIA 45/43) in **l**, posterior and **m**, right lateral view. Right humerus of *Yarasuchus* (ISIR 334 53) in **n**, anterior and **o**, posterior views. **p**, Right ulna of *Yarasuchus* (ISIR 334) in anterior view. **q**, Trunk vertebra of *Yarasuchus* (ISIR BIA 45/43) in left lateral view. Posterior cervical vertebrae of *Yarasuchus* (ISIR BIA 45/43) in **r**, posterior and **s**, right lateral view. **t**, Triple-headed rib of *Yarasuchus* (ISIR BIA 45) in anterior view**. u** Original condition of a cervical vertebra (from Huene 1942) of *Spondylosoma absconditum* (GPIT 479/30) compared to that of the **x**, the current condition of the same vertebra. Original condition of a more posterior cervical vertebra (from Huene 1942) in **v**, left lateral and **w**, anterior views compared to that of the current condition of the same vertebra in **y**, left lateral view. **z**, Trunk vertebra in posterior view. **aa**, Second sacral vertebra in dorsal view. Right scapula in **bb**, lateral and **cc**, posterior views. a., articulates with; ain, anteriorly inclined anterior margin of the neural spine; as, astragalus; ct, calcaneal tuber; dp, deltopectoral crest; fi, fibula; hy, hyposphene; mic, M. iliotrochantericus caudalis scar; mie, M. iliofemoralis externus scar; pr, posterolateral; r, ridge. Scales = 1 cm. GPIT, Paläontologische Sammlung der Universität Tübingen, Tübingen, Germany; ISI, Indian Statistical Institute, Kolkata, India; PIN, Borissiak Paleontological Institute of the Russian Academy of Sciences, Moscow, Russia. Outline of Africa and Tanzania obtained from Google maps.

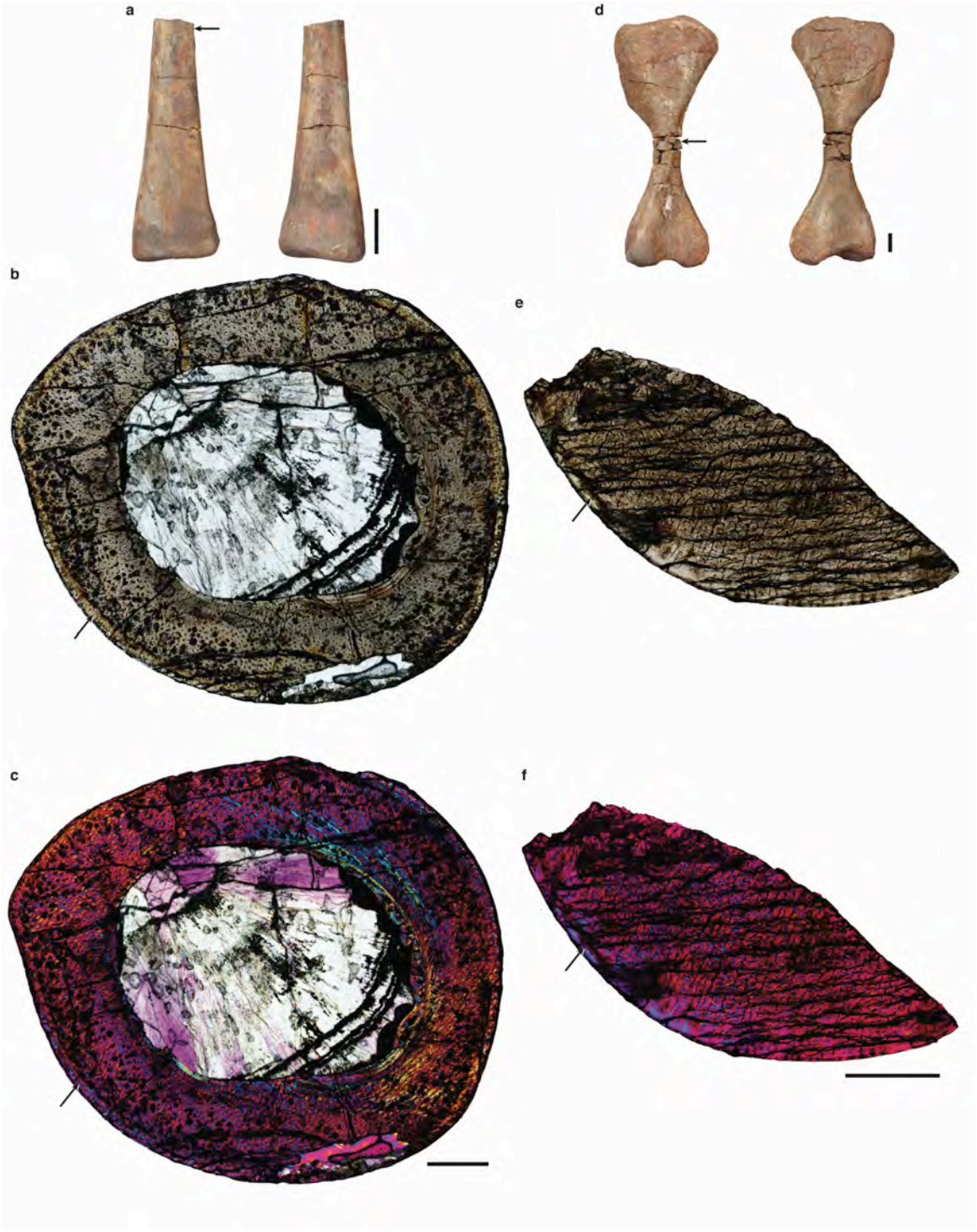

Extended Data Figure 2. Histological sections of the limb bones of *Teleocrater rhadinus* gen et sp. nov. a, Right fibula (NMT RB 488) in lateral (left) and medial (right) views. **b,** Photo of the histological section of the fibula (NMT RB 488) in regular

transmitted light (brightfield) (1 plane polarizer) and **c**, photo of the same section using a full wave retarder (lambda = 530 nm). **d**, Left humerus (NMT RB476) in posterior (left) and anterior (right) views. **e**, Photo of a partial histological section of the humerus (NMT RB476) in regular transmitted light (brightfield) (1 plane polarizer) and **f**, photo of the same section using a full wave retarder (lambda = 530 nm). Scale = 1 mm. Arrows indicate where each element was sampled in **a** and **d** and indicate growth marks in the outer cortex in **c**-**d**, **e**-**f**.

Extended Data Figure 3. The relationships of *Teleocrater rhadinus* gen et sp. nov. among archosauriforms from the Nesbitt (2011) dataset. Strict consensus of 36 Most Parsimonious Trees (Tree Length = 1374; Consistency Index = 0.3559; Retention Index = 0.7807). Bremer support values (first), absolute (second), and GC (third) bootstrap frequencies presented at each branch.

Extended Data Figure 4. The relationships of *Teleocrater rhadinus* gen et sp. nov. among archosauriforms from the Ezcurra (2016) dataset. Strict consensus of 4 Most Parsimonious Trees (Tree Length = 2684; Consistency Index = 0.2955; Retention Index = 0.6284). Bremer support values (first), absolute (second), and GC (third) bootstrap frequencies presented at each branch.

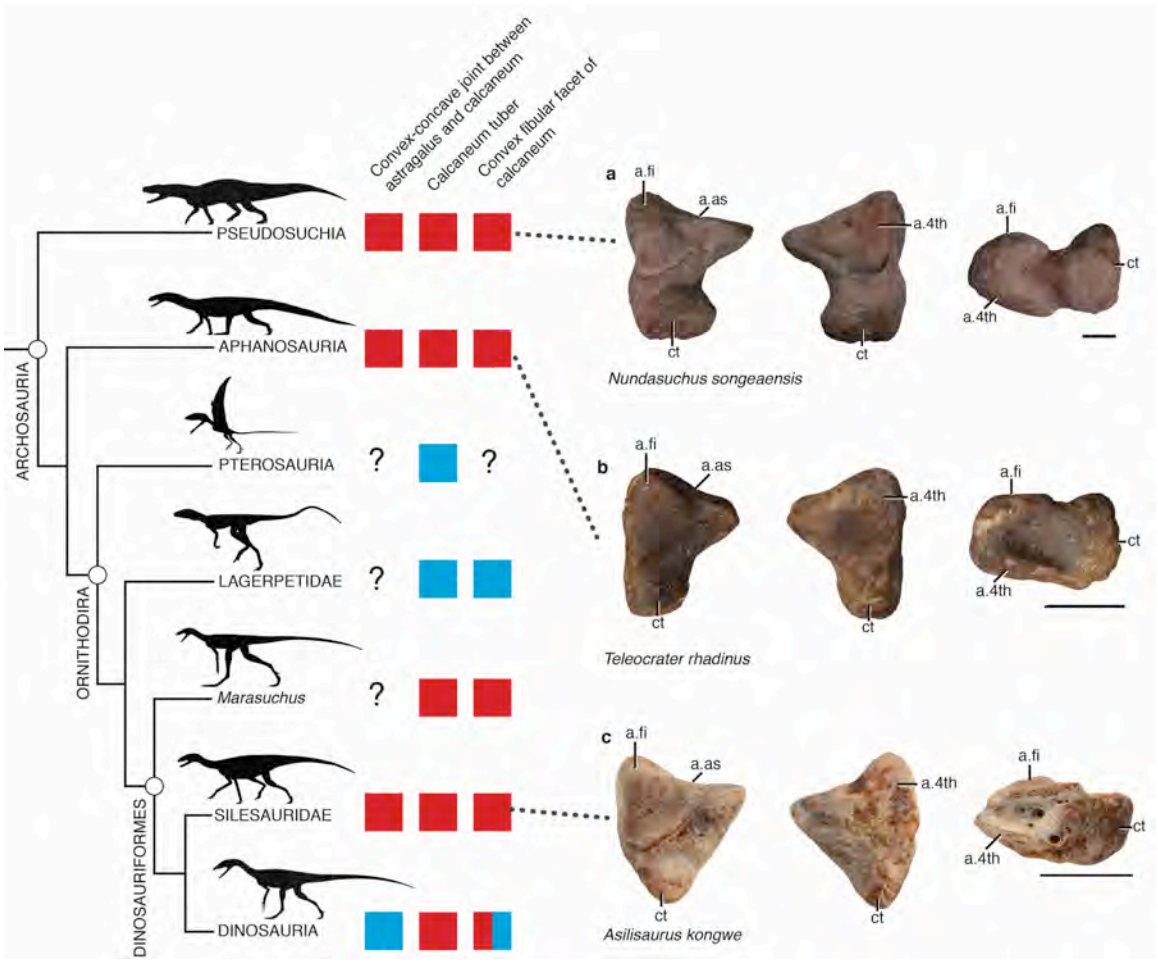

Extended Data Figure 5. Phylogeny of early Avemetatarsalia illustrating the character distributions of the components of the 'crocodile-normal' ankle configuration and showing that this ankle type was plesiomorphic for Archosauria, Avemetatarsalia, and possible less inclusive clades within Avemetatarsalia (e.g., Dinosauriformes). a, Left calcaneum of the pseudosuchian *Nundasuchus songeaensis* (NMT RB48). **b**, Right calcaneum of the aphanosaur *Teleocrater rhadinus* gen et sp. nov. (reversed) (NMT RB490). **c**, Left calcaneum of the dinosauriform silesaurid *Asilisaurus kongwe* (NMT RB159). Proximal view (left), distal view (middle), and lateral view (right). Scales = 1 cm. red = character state present; blue = character state absent; red and blue = basal condition could be either; ? = unknown condition. See Figure 3 for silhouette

sources. 4th, fourth tarsal; a., articulates with; as, astragalus; ct, calcaneal tuber; fi, fibula.

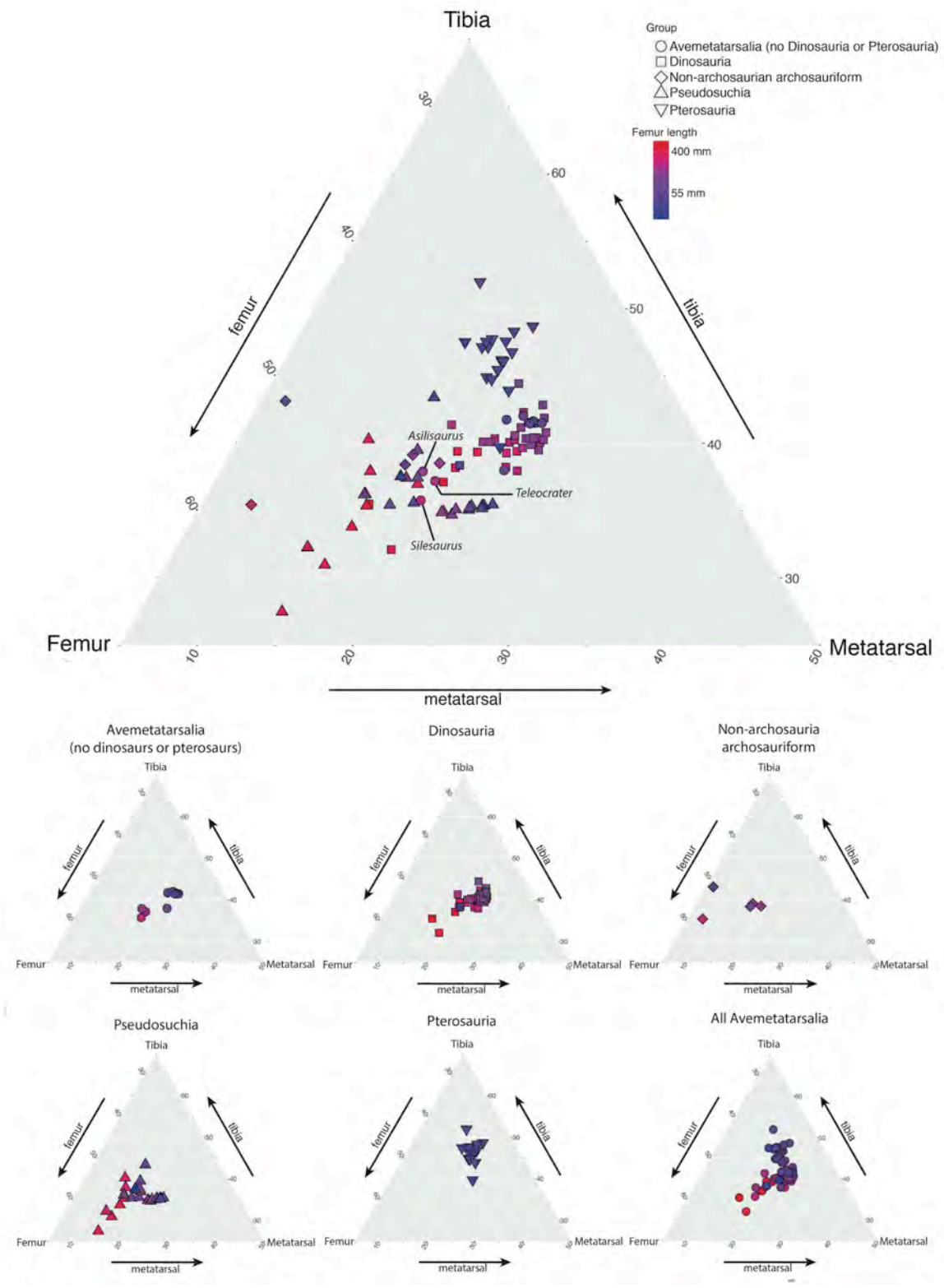

Extended Data Figure 6. Ternary diagrams of measurements of the hindlimb elements (femur, tibia, and longest metatarsal) of archosauriforms. Colour of data

points relates to femoral length.

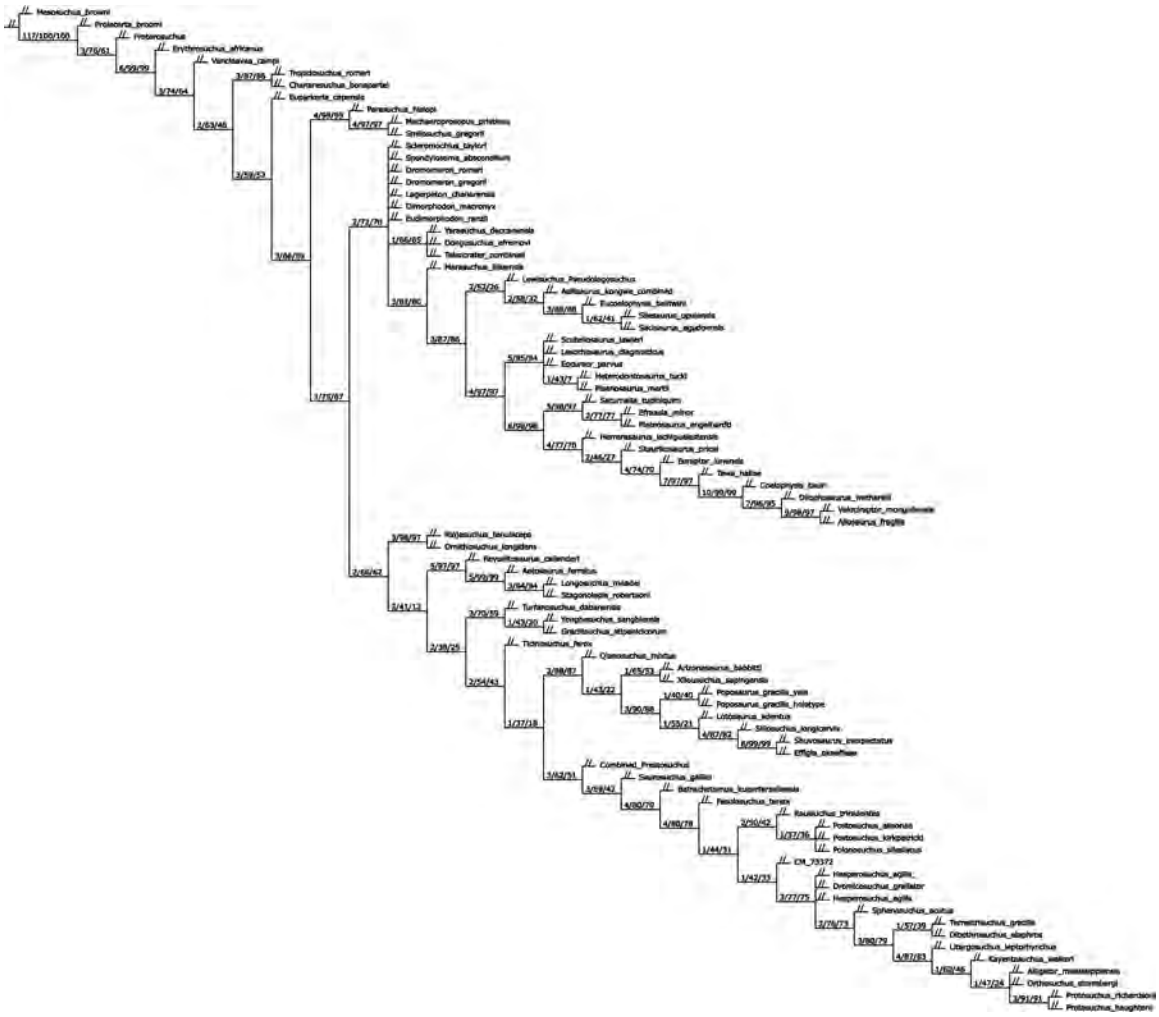

Extended Data Figure 7. The relationships of *Scleromochlus taylori* among archosauriforms from the Nesbitt (2011) dataset. Strict consensus of 792 Most Parsimonious Trees (Tree Length = 1378; Consistency Index = 0.3549; Retention Index = 0.7803) (see Supplementary Information). Bremer support values (first), absolute (second), and GC (third) bootstrap frequencies presented at each branch.

Extended Data Figure 8. The relationships of *Scleromochlus taylori* among archosauriforms from the Ezcurra (2016) dataset. Strict consensus of 4 Most Parsimonious Trees (Tree Length = 2693; Consistency Index = 0.2945; Retention Index = 0.6280) (see Supplementary Information). Bremer support values (first), absolute (second), and GC (third) bootstrap frequencies presented at each branch.

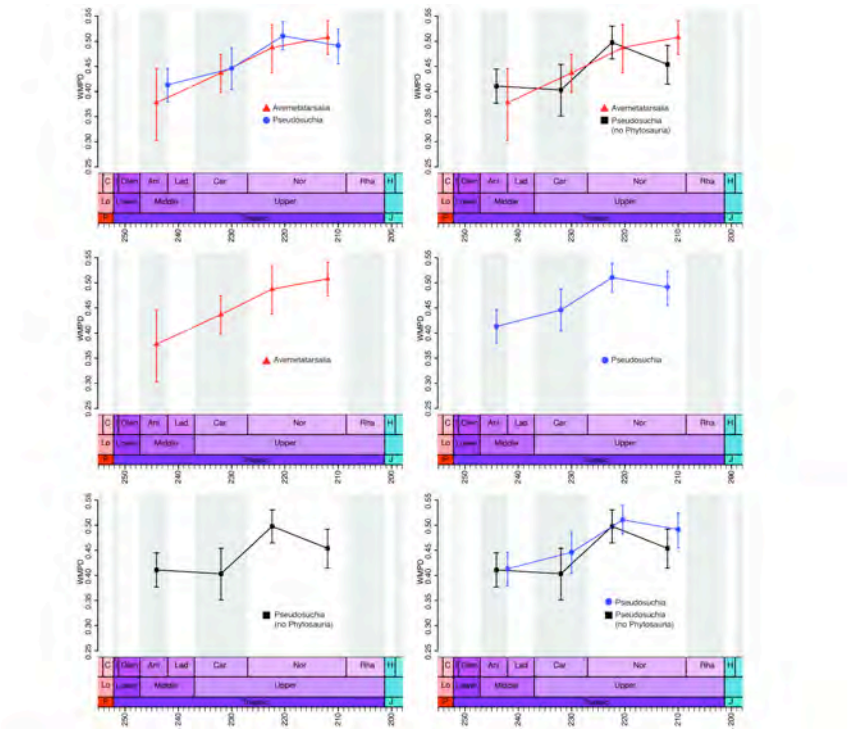

Extended Data Figure 9. Disparity estimates for major archosaur groups and time intervals (weighted mean pairwise dissimilarity [WMPD]). Ani, Anisian; C, Changhsingian; Car, Carnian; H, Hettangian; I, Induan; J, Jurassic; Lad, Ladinian; Lo, Lopingian; Nor, Norian; Olen, Olenekian; P, Permian; Rha, Rhaetian.

Extended Data Figure 10. New character illustrations for the phylogenetic analysis (see Supplemental Information). Archosaurian iliac comparisons for character 414 in the modified Nesbitt (2011) dataset: left ilium of *Teleocrater rhadinus* (NHMUK PV R6795) in **a**, lateral view; right ilium of *Asilisaurus kongwe* (NMT RB159) in **b**, lateral view; left ilium of *Batrachotomus kupferzellensis* (SMNS 80273) in **c**, lateral view. Avemetatarsalian fibula comparisons for character 415 in the modified Nesbitt (2011) dataset: left fibula of *Teleocrater rhadinus* (NHMUK PV R6795) in **d**, lateral and **e**, posterior views; left fibula of *Asilisaurus kongwe* (NMT RB159) in **f**, lateral and **g**,

posterior views; Arrow highlights the posterior ridge, character 415 state 1. Archosauriform femoral comparisons for character 417 in the modified Nesbitt (2011) dataset: right femur of *Erythrosuchus africanus* (NHMUK PV R3592) in **h**, ventral view; right femur of *Teleocrater rhadinus* (NHMUK PV R6795) in **i**, posteromedial view. White dotted region highlights character 417, state 1. Avemetatarsalian second primordial sacral comparisons for character 416 in the modified Nesbitt (2011) dataset: second primordial sacral vertebra of *Teleocrater rhadinus* (NMT RB519) in **j**, ventral and **k**, posterior views. The second primordial sacral vertebra of *Asilisaurus kongwe* (NMT RB159) in **l**, ventral and **m**, dorsal views. Arrow highlights the posterior process of the sacral rib, character 416, state 1. SMNS, Staatliches Museum für Naturkunde Stuttgart Scales: **a**–**g**, **i**–**m**, 1 cm; **h**, 5 cm.

SUPPLEMENTARY INFORMATION

The earliest bird-line archosaurs and the assembly of the dinosaur body plan

Sterling J. Nesbitt[1*], Richard J. Butler[2], Martín D. Ezcurra[2,3], Paul M. Barrett[4], Michelle R. Stocker[1], Kenneth D. Angielczyk[5], Roger M.H. Smith[6,7] Christian A. Sidor[8], Grzegorz Niedźwiedzki[9], Andrey G. Sennikov[10,11], Alan J. Charig[†4]

Extended Systematic Palaeontology

Archosauria Cope, 1869 *sensu* Gauthier and Padian, 1985

Avemetatarsalia Benton, 1999

Terminology comments—Prior to this contribution, there has been little need for a name for the bird stem lineage, which includes all archosaurs more closely related to Aves than to Crocodylia, because the node-based name Ornithodira includes the previously basalmost diverging group, Pterosauromorpha, as a specifier in its definition (Gauthier 1986). However, our phylogenetic analyses recovered *Teleocrater rhadinus* and related taxa (Aphanosauria) outside Ornithodira but closer to Aves than to Crocodylia. Accordingly, we use the previously proposed stem-based clade name Avemetatarsalia to encompass all archosaurs more closely related to Aves than to Crocodylia, following Benton (1999). We note that the less commonly used name Ornithosuchia (Gauthier 1986) also encompasses the same phylogenetic content. The name Ornithosuchia was erected prior to Avemetatarsalia (Senter 2005), but at present no formal system of priority exists for phylogenetic definitions above the family level (prior to the proposed implementation of the PhyloCode). However, it is now clear that the clade Ornithosuchidae, a key component of Gauthier's conception of Ornithosuchia, is part of Pseudosuchia and is not closer to birds than to crocodylians (e.g. Nesbitt 2011, and references therein). Additionally, Avemetatarsalia has been more commonly used in the latest phylogenetic analyses including early archosaurs (Brusatte et al. 2010a; Nesbitt 2011; Ezcurra 2016). Therefore, we prefer to use Avemetatarsalia instead of Ornithosuchia.

Aphanosauria clade nov.

Extended Diagnosis—Epipophyses present on post-axial anterior cervical vertebrae (Nesbitt 2011:character 186, state 1; abbreviated to e.g. 'N186-1' hereafter; and Ezcurra 2016: character 336, state 1; abbreviated to e.g. 'E336-1' hereafter); dorsal end of neural spines of cervical vertebrae blade-like, but with adjacent, rounded expansions with a rugose texture (N191-3, ambiguous when *Dongusuchus efremovi* is included); anterior and middle postaxial cervical neural spines with a strong anterior overhang (E343-1); posterior cervical vertebrae with an articulation surface just dorsal to the parapophysis (= divided parapophysis of Nesbitt 2011) (N193-1; E314-1); dorsally opening pit lateral to the base of the neural spine of trunk vertebrae (E361-1); elongated deltopectoral crest of the humerus greater than 30% the length of the shaft (N230-1); wide distal end of the humerus greater than 30% of humerus length (N235-1); extensive contact between the

ischia on the midline but the dorsal margins are separated (E485-1; N191-1, but ambiguous); rounded outline of the posteroventral portion of the ischium (N293-1); longitudinal groove on the dorsal surface of shaft of the ischium (E484-1); femur with a scar for M. iliofemoralis externus near the proximal surface (homologous with the anterior trochanter in dinosauromorphs) (N308-1; E520-1); proximal surface of the femur with a straight transverse groove (N314-1; E495-1); distal articular surface of the femur concave (E512-2); calcaneal tuber taller than broad (N376-0).

Teleocrater rhadinus gen. et sp. nov.

Differential Diagnosis—*Teleocrater rhadinus* differs from all other archosauriforms except *Yarasuchus deccanensis* and *Dongusuchus efremovi* in the possession of the following combination of character states (*= possible autapomorphy): anterior cervical vertebrae with large, sub-elliptical neural canal openings, in which the anterior neural canal opening has a mediolaterally oriented long axis, whereas the posterior neural canal opening is elliptical with the long axis oriented dorsoventrally*; anterior cervical vertebrae at least 1.5 times longer than anterior to middle trunk vertebrae; preacetabular process of the ilium arcs medially to create a distinct pocket on the medial surface; small concave ventral margin of the ischial peduncle of the ilium; long iliofibularis crest of the fibula; anterior edge of the proximal portion of fibula curved laterally. *Teleocrater rhadinus* differs from *Yarasuchus deccanensis* by a more posteriorly directed glenoid of the scapula. The femur of *Teleocrater rhadinus* and the holotypic femur of *Dongusuchus efremovi* are very similar and only differ in a few minor aspects. The femur of *Teleocrater rhadinus* differs from that of *Dongusuchus efremovi* by the presence of a more rounded lateral portion of the proximal section in anterolateral view, the medial surface of the proximal end is concave, the ratio of total femoral length to minimum midshaft diameter is lower (~12), and the posteromedial tuber of the proximal portion is convex mediolaterally instead of flattened as in *Dongusuchus efremovi*.

Referred Material—Left maxilla (NMT RB495); right frontal (NMT RB496); left quadrate (NMT RB493); braincase (NMT RB491); axis (NMT RB504); anterior cervical vertebrae (NMT RB505, NMT RB506); middle cervical vertebrae (NMT RB511, NMT RB512); posterior cervical vertebra (NMT RB514); anterior trunk vertebra (NMT RB500); posterior trunk vertebrae (NHMUK PV R6796, NMT RB516); second sacral vertebra (NMT RB519); right scapula (NMT RB480); left humeri (NMT RB476; NMT RB477); distal half of left humerus (NHMUK PV R6796); left ulnae (NMT RB485, NMT RB486); metacarpal (NMT RB484); left ilium (NMT RB489); left ischium (NMT RB479); right femur (NMT RB498); left tibia (NMT RB481); right fibulae (NMT RB482, NMT RB488); right calcaneum (NMT RB490).

Justification for association and assignment of the referred specimens of *Teleocrater rhadinus*

The holotype of *Teleocrater rhadinus* consists of a partial, associated (but disarticulated) skeleton, including: four cervical, seven trunk, and 17 caudal vertebrae; two rib fragments, one from the cervical region and one from the trunk region; partial right scapula; partial coracoid; complete right radius and ulna; partial left ilium; both

femora; both tibiae; left fibula; two proximal ends of metatarsals; isolated phalanges; and associated fragments (Charig 1956). The specimen was collected in a small area by F.R. Parrington in 1933 near the confluence of the Mkongoleko and Rutikira rivers, Ruhuhu Basin, southern Tanzania (Parrington's field number 48b). The exact locality is not known but was mapped as locality B9 of Stockley (1932) by F. R. Parrington and recorded as "1/2 hours march west village of Mkongoleko. South of river Mkongoleko" (field notes of F.R. Parrington, 1933, UMZC). We interpret all of the specimens that make up the holotype as pertaining to one individual because all of the elements 1) were found together (field notes of F.R. Parrington, 1933, UMZC), 2) have similar preservation, 3) lack duplication, 4) are consistent in relative size for a single individual, and 5) are all nearly identical to those in the hypodigm of *Yarasuchus deccanensis* (Sen 2005). Other referred specimens (e.g. NHMUK PV R6796) were collected from the same area as the holotype, but were far enough from the holotype that Parrington considered them to represent another individual.

In 2015, part of our team discovered a bonebed locality (see below) in the lower portion of the Lifua Member of the Manda Beds, within 1 km of the mapped position of Stockley's (1932) locality B9. Given the proximity of the holotype locality and the 2015 locality (Z183), it is possible that the holotype of *Teleocrater rhadinus* was collected from the same outcrop, or even the same bonebed, more than 70 years earlier. The referred specimens of *Teleocrater rhadinus* with NMT numbers were found together in a ~15 cm horizon within a thicker accumulation of vertebrates (see below). All specimens of *Teleocrater rhadinus* were found disarticulated and mixed with the remains of an allokotosaurian archosauromorph that is easily distinguishable from the elements assigned to *Teleocrater rhadinus*. Elements of *Teleocrater rhadinus* from this horizon can be recognised by their similarity to the holotype and *Yarasuchus deccanensis*, similar preservation, smaller size than the allokotosaurian remains, and by the possession of character states found in archosauriforms (e.g. presence of an antorbital fenestra). At least three individuals of *Teleocrater rhadinus* are present based on overlapping elements and clear differences in size. We assign each element from Z183 independently to *Teleocrater rhadinus* based on 1) direct overlap of skeletal elements with the holotype, 2) direct overlap of skeletal elements with its sister taxon, *Yarasuchus rhadinus*, or 3) if the referred element is not present in the holotype or in *Yarasuchus rhadinus*, we assigned it based on its similar size to other referred elements of *Teleocrater rhadinus,* its style of preservation in comparison with the other confirmed elements, and the phylogenetic consistency of a position within Archosauriformes, Archosauria, and Avemetatarsalia.

Supplementary Table S1. Measurements of the vertebrae of the holotype of *Teleocrater rhadinus* (NHMUK PV R6795). The proposed order of vertebrae within the column follows that proposed by Charig (1956) and reflects some uncertainly in the exact positions of the vertebrae. Abbreviations: Cd, caudal vertebra; CHA, height of anterior centrum articular surface; CHP, height of posterior centrum articular surface; CL, centrum length; CMW, centrum minimum transverse width; Cv, cervical vertebra; CWA, width of anterior centrum articular surface; CWP, width of posterior centrum articular surface; D, 'dorsal' (=trunk) vertebra. All measurements are provided in mm. Measurements that are too distorted/incomplete to include are denoted by a hyphen.

Vertebra	CL	CHA	CWA	CHP	CWP	CMW
CvA	53	-	-	14	13	8
CvB	32	14	15	14	15	7
DA	26	14	15	15	15	7
DB	25	14	15	15	16	7
DC	24	14	17	13	17	8
DD	25	13	15	13	15	7
DE	28	14	16	13	16	7
DF	30	13	17	14	18	6
DG	26	14	16	15	18	8
DH	21	14	17	14	17	9
DI	22	17	20	15	18	10
DJ	21	16	-	17	18	9
DK	21	16	17	16	17	10
CdA	24	14	13	14	13	7
CdB	23	13	12	12	12	7
CdC	23	12	12	11	11	6
CdD	23	11	11	10	11	6
CdE	23	11	11	11	11	5
CdF	23	10	10	11	10	5
CdG	24	9	9	10	9	5
CdH	25	10	9	12	9	5
CdI	23	10	10	10	10	5
CdJ	22	10	10	10	10	6
CdK	22	9	9	9	9	5
CdL	25	10	10	10	10	6

CdM	24	9	9	9	9	5
CdN	25	10	10	8	9	5
CdO	22	7	6	6	7	3

Supplementary Table S2. Measurements of the limb elements of the holotype of *Teleocrater rhadinus* (NHMUK PV R6795). All measurements are provided in mm.

Element/measurement	
Right radius	
Length	88
Length of proximal end	16
Length of distal end	12
Midshaft circumference	22
Right ulna	
Length	92
Length of proximal end	19
Length of distal end	13
Midshaft circumference	22
Right femur	
Length	170
Length of proximal end	35
Length of distal end	35
Midshaft circumference	51
Left femur	
Length	170
Length of proximal end	35
Length of distal end	35
Midshaft circumference	53
Right tibia	
Length	145
Length of proximal end	30
Length of distal end	20
Midshaft circumference	40

Left tibia	
Length	145
Length of proximal end	30
Length of distal end	21
Midshaft circumference	41
Left fibula	
Length	143
Length of proximal end	20
Length of distal end	17
Midshaft circumference	27

Supplementary Table S3. Known material of *Teleocrater rhadinus*.

Element	Specimen number	Holotype	Referred, not in holotype, but in *Yarasuchus*	Referred, not in holotype or *Yarasuchus*
maxilla	NMT RB495			X
quadrate	NMT RB493			X
frontal	NMT RB496			X
braincase	NMT RB491			X
axis	NMT RB504		X	
anterior cervical vertebra	NMT RB505	X	X	
mid cervical vertebra	NMT RB511		X	
posterior cervical vertebra	NMT RB514	X	X	
anterior trunk vertebra	NMT RB500	X	X	
middle trunk vertebra	NHMUK PV R6795	X		
posterior trunk vertebra	NMT RB516	X	X	
second sacral	NMT RB519		X	
middle caudal vertebrae	NHMUK PV R6795	X		
distal caudal vertebrae	NHMUK PV R6795	X		
scapula	NMT RB480	X	X	
coracoid	NHMUK PV R6795	X		
humerus	NMT RB476		X	
ulna	NMT RB485	X	X	
radius	NHMUK PV R6795	X		
metacarpal	NMT RB484			X
ilium	NMT RB489	X	X	
ischium	NMT RB479		X	
femur	NMT RB498	X	X	
tibia	NMT RB481	X	X	
fibula	NMT RB482	X		
calcaneum	NMT RB490		X	
metatarsals	NHMUK PV R6795	X		
phalanges	NHMUK PV R6795	X		

Description of sedimentary environment and taphonomy of the referred specimens of *Teleocrater rhadinus* and the associated assemblage

The referred specimens of *Teleocrater rhadinus* were found at locality Z183 in an erosion gully floored by medium-grained pinkish-gray, trough cross-bedded sandstone containing scattered, well-rounded, extrabasinal quartz pebbles up to 2cm in diameter. The upper contact of this interpreted channel-fill shows sloping wedge-shaped stringers of medium-grained sandstone interdigitating with an overlying dark reddish-brown/olive grey mottled sandy siltstone, a characteristic feature of inner-bank point-bar deposits (Diaz-Molina 1993).

The main bone-on-bone multi-taxon bonebed occurs 1.5m above the upper point bar facies in a narrow 45cm-thick interval of alternating tabular sandstone/siltstone beds with minor stringers of dark brown claystone. Here, numerous large and small partially articulated, disarticulated, and fragmented bones of dicynodonts, cynodonts (Wynd et al. 2016), and archosauromorphs, including *Teleocrater rhadinus* (Supplementary Table S4) occur in two discrete taphonomic modes. The larger bones are mostly of the dicynodont *Dolichuranus* sp. (e.g. NMT RB554; Kammerer et al. unpublished data) and the cynodont *Cynognathus*, and they are commonly semi-articulated and closely-associated, suggesting minimal transportation from site of death. They are hosted by a bed of white/pinkish-grey, mottled, fine-grained, silty-sandstone with dark brown mudstone chips and pebbles that immediately overlies a basal lag of smaller, more fragmented, and taxonomically diverse bones of archosauromorphs (including *Teleocrater rhadinus,* NMT RB498, and an allokotosaurian, NMT RB550), temnospondyls (NMT RB551), and another small reptile (NMT RB552).

The bonebed succession of upward coarsening, thin tabular traction-current sandstone sheets, bounded by pedogenically-modified mudrocks is interpreted as a distal crevasse splay (Smith 1993). In such a setting, the bone accumulation mechanism was likely shallow sheetwash events that intermittently swept the floodplain and dumped the bedload into temporary standing water bodies to be subsequently buried by the prograding crevasse splay complex (Smith et al. 1989). The larger associated carcasses were transported only once, whereas the underlying carpet of fragmented and abraded bones had been mobilised several times by successive flood events before final burial. Before significant compaction had taken place, the dicynodont remains in the more arenaceous matrix had become thickly encrusted with calcareous nodular material. In contrast most of the lag deposit bones within finer-grained matrix are free of surface mineralization.

Supplementary Table S4. The lower and middle–upper tetrapod assemblages of the Lifua Member of the Manda Beds (Middle Triassic), Ruhuhu Basin, southern Tanzania.

Taxon	Figure 1 number	Voucher	Source
Stagonosuchus nyassicus	1	GPIT/RE/3831	von Huene 1938
Asilisaurus kongwe	2	NMT RB9	Nesbitt et al. 2010
Ruhuhuaria reiszi	3	UMCZ T997	Tsuji et al. 2013b
'Stanocephalosaurus' pronus	4	UMZC T289	Howie 1970
Mandagomphodon hirschsoni	5	NHMUK PV R8577	Hopson 2014
Undescribed procolophonid	6	NMT RB167	Tsuji et al. 2013a
Stenaulorhynchus stockleyi	7	NMT RB186	von Huene 1938
'*Rechnisaurus cristarhynchus*'	8	NHMUK PV R11995	Cox 1991
Angonisaurus cruickshanki	9	NHMUK PV R9732	Cox and Li 1983
Parringtonia gracilis	10	NHMUK PV R8646	von Huene 1939
'*Ruhuhuungulasaurus croucheri*'	11	NHMUK PV R12710	Larkin 1994
Scalenodon angustifrons	12	UMZC T907	Crompton 1955
Tetragonias njalilus	13	GPIT K292	von Huene 1942

Cricodon metabolus	14	UMZC T905	Crompton 1955
Asperoris mnyama	15	NHMUK PV R36615	Nesbitt et al. 2013b
Sangusaurus parringtonii	16	UMZC T1226	Cruickshank 1986
Mandagomphodon attridgei	17	NHMUK PV R8578	Crompton 1972
Nundasuchus songeaensis	18	NMT RB48	Nesbitt et al. 2014
'*Mandasuchus tanyauchen*'	19	NHMUK PV R6792	Butler et al. unpublished data
'*Stanocephalosaurus*' *pronus*	20	UMZC T288	Howie 1970
Hypselorhachis mirabilis	21	NHMUK PV R16586	Butler et al. 2009
Teleocrater rhadinus	22	NHMUK PV R6795	This paper
Cynognathus	23	NMT RB459	Wynd et al. 2016
Undescribed small reptile	24	NMT RB553	This paper
Dolichuranus sp.	25	NMT RB554	Kammerer et al. unpublished data
Undescribed allokotosaurian	26	NMT RB550	This paper

Further comparisons with closely related taxa

1. *Nyasasaurus parringtoni*

Teleocrater rhadinus, a basal avemetatarsalian, and *Nyasasaurus parringtoni,* a likely dinosauriform or dinosaur (Nesbitt et al. 2013a), are both from the Lifua member of the Manda Beds. *Teleocrater rhadinus* is from the lower portion of the Lifua Member, whereas the exact stratigraphic position of *Nyasasaurus parringtoni* is unknown. *Nyasasaurus parringtoni* is known only from incompletely preserved cervical, trunk, and sacral vertebrae and a humerus (Nesbitt et al. 2013a) and some of the morphologies of those bones are similar to those of *Teleocrater rhadinus*. Therefore, in the following sections we compare overlapping elements of *Teleocrater rhadinus* and *Nyasasaurus parringtoni* and critically analyze the question 'is *Teleocrater* a young *Nyasasaurus parringtoni*'?

The holotype humerus of *Nyasasaurus parringtoni* (NHMUK PV R6856) and two complete referred humeri (NMT RB476; NMT RB477) of *Teleocrater rhadinus* can be compared directly. Both taxa share an elongated deltopectoral crest with poorly developed proximal and distal surfaces. The elongated deltopectoral crest is a rare character state outside of dinosaurs, but does occur in some more distantly related taxa (e.g. *Erythrosuchus africanus*; Gower 2003). A crest on the dorsolateral surface of the deltopectoral crest is much more pronounced in *Nyasasaurus parringtoni*, whereas the feature is present, but much fainter, in the two humeri of *Teleocrater rhadinus*. In *Nyasasaurus parringtoni*, the deltopectoral crest is nearly sigmoidal in lateral view where the distal portion of the crest flares laterally; the deltopectoral crest is simply expanded anterolaterally in *Teleocrater rhadinus* with no lateral deflection of the apex. Furthermore, *Teleocrater rhadinus* lacks a small notch distal to the deltopectoral apex that is present in *Nyasasaurus parringtoni*. The humeri of *Teleocrater rhadinus* lack a pronounced broad fossa on the anterior surface that connects with the proximal surface in *Nyasasaurus parringtoni*. Finally, the medial tuberosity of *Teleocrater rhadinus* is distinct and shifted from the humeral head, whereas the medial tuberosity and humeral head are continuous in *Nyasasaurus parringtoni*.

The histologies of the humerus of *Nyasasaurus parringtoni* and *Teleocrater rhadinus* differ in several respects. The vascularity of *Nyasasaurus parringtoni* is higher in the inner and middle cortex and there are more anastomoses in these regions compared to the same area in *Teleocrater rhadinus*. Additionally, the vascularity is composed of more radial canals in *Teleocrater rhadinus* than in *Nyasasaurus parringtoni*. The outer portion of the smaller humerus of *Teleocrater rhadinus* has a growth mark (i.e. line of arrested growth [LAG]) in the outermost cortex, whereas the larger humerus of *Nyasasaurus parringtoni* lacks growth marks (Nesbitt et al. 2013a). The absence of LAGs in *Nyasasaurus parringtoni* may suggest that it was a younger individual than that of *Teleocrater rhadinus*, although it was bigger, or that it had uninterrupted growth during its life.

The holotype of *Nyasasaurus parringtoni* (NHMUK PV R6856) possesses three sacral vertebrae (Nesbitt et al. 2013a) as identified by the presence of sacral ribs coossified to the centra. Only the second sacral vertebra was recovered in *Teleocrater* (NMT RB519). Comparisons with the sacrum of *Nyasasaurus* are difficult because its second primordial sacral is highly incomplete. However, the second primordial sacral centrum of *Nyasasaurus parringtoni* is slightly more robust than that of *Teleocrater rhadinus* (NMT RB519) and the posterior articular rim of *Teleocrater rhadinus* is not as ventrally extended as it is in *Nyasasaurus parringtoni*.

The presence of three sacral vertebrae in *Nyasasaurus parringtoni* (NHMUK PV R6856) supports the distinction of *Teleocrater* and *Nyasasaurus* based on the number of sacral vertebrae positions inferred for the holotype of *Teleocrater rhadinus* (NHMUK PV R6795). The ilium of *Teleocrater* has positions for the attachment of the first and second primordial sacral ribs only. The posterior portion of the ilium of *Teleocrater rhadinus* (NHMUK PV R6795) is broken; however, the scar for the rib of the second primordial sacral vertebra is present on the preserved portion. In contrast, the iliac morphology inferred for *Nyasasaurus parringtoni* should have at least three sacral vertebra scars in the area homologous to that preserved in *Teleocrater rhadinus.*

The holotype of *Nyasasaurus parringtoni* (NHMUK PV R6856) lacks cervical vertebrae, but Nesbitt et al. (2013a) referred several elongated cervical vertebrae to this taxon based on their shared character states with dinosaurs and their close relatives. These elongated cervical vertebrae (SAM-PK-K10654) are similar in length to those of the anterior cervical vertebrae of *Teleocrater rhadinus*, but differ in several important features. The cervical vertebrae referred to *Nyasasaurus parringtoni* have the following character states that are not present in the anterior cervical vertebrae of *Teleocrater rhadinus*: very deep fossae on the posterior side of the lateral surface of the neural canal (df in Fig. S8 of Nesbitt et al. 2013a); wide neural spines at the posterior portion of the neural arch; deep fossae lateral to the neural canal in anterior view; and well-separated diapophyses and parapophyses. The presence of deep fossae on the lateral side of the neural arch and adjacent to the neural canal are important phylogenetic character states that place *Nyasasaurus parringtoni* near or within Dinosauria, and these character states are clearly absent in the anterior cervical vertebrae of *Teleocrater rhadinus*. If the referred cervical vertebrae (SAM-PK-K10654) of *Nyasasaurus parringtoni* are ultimately removed from that taxon, these vertebrae are different enough that they would not pertain to *Teleocrater rhadinus*.

The morphology and histology of the holotype and referred specimens of

Nyasasaurus parringtoni (NHMUK PV R6856; SAM-PK-K10654, cervical vertebrae) are all distinct from the known elements of *Teleocrater rhadinus*. Although we know very little about the morphology of *Nyasasaurus parringtoni*, those comparisons that are possible demonstrate that the two taxa are different.

2. *Yarasuchus deccanensis*

Sen (2005) described *Yarasuchus deccanensis* from the lower Middle Triassic Yerrapalli Formation (central India) based on the disarticulated bones of at least two similarly-sized individuals (Extended Data Fig. 1) found in association with two individuals of the allokotosaurian *Pamelaria dolichotrachela*. Sen (2005) interpreted *Yarasuchus deccanensis* as a long-necked, gracile rauisuchian pseudosuchian, and Brusatte et al. (2010a) subsequently recovered it as a poposauroid in a cladistic analysis. Desojo (in Lautenschlager and Desojo 2011) suggested that *Yarasuchus deccanensis* was a chimera composed of a 'rauisuchian' and a 'prolacertiform'. More recently, Ezcurra (2016) did not find non-crocopodan archosauromorph (i.e. 'prolacertiform') or non-crocodylomorph paracrocodylomorph (i.e. 'rauisuchian') apomorphies in the available bones of *Yarasuchus deccanensis* and considered most of the bones (i.e. maxilla + postcranial elements) to belong to a single species. Ezcurra (2016) recovered *Yarasuchus deccanensis* as more closely related to *Dongusuchus efremovi* than to other archosauromorphs, and this clade fell among the most basal eucrocopodan archosauriforms.

Based on a first-hand revision of the holotype and referred bones of *Yarasuchus deccanensis*, and the new data provided by *Teleocrater rhadinus*, we provide some novel anatomical details for the Indian species that shed light on its phylogenetic relationships.

Sen (2005) referred to *Yarasuchus deccanensis* a partial premaxilla and maxilla attached to each other, a right maxilla and jugal, a left quadrate coossified with the ventral end of the quadratojugal, a right squamosal, and both pterygoids. The two maxillae belong to the right side of the skull and possess consistent dental morphology. The maxilla attached to the premaxilla is heavily crushed, covered with glue, and seems to have belonged to a larger animal than that represented by the holotype of *Yarasuchus deccanensis.* The other right maxilla is well preserved and lacks the ascending process. This bone differs from that of *Teleocrater rhadinus* in the absence of an antorbital fossa on the horizontal process and the tapering posterior end of this process. Instead, this maxilla closely resembles that of an undescribed allokotosaurian found in the same bonebed as *Teleocrater rhadinus* (SJN pers. obs.). The fact that *Yarasuchus deccanensis* was found in close association with allokotosaurian bones (*Pamelaria*) suggests that the maxilla found with *Yarasuchus* probably belongs to a member of this clade of basal archosauromorphs.

The jugal and coossified quadratojugal-quadrate described by Sen (2005) are considered as indeterminate bones herein. The bone originally identified as a right squamosal is reinterpreted as a right postorbital, but it seems to belong to a bigger individual than the holotype of *Yarasuchus deccanensis*. The pterygoid fits approximately with the size and morphology expected for the species.

The postcranial bones that comprise the holotype and referred specimens of *Yarasuchus deccanensis* are congruent with each other in morphology and size and with that expected based on the anatomy of *Teleocrater rhadinus*. As a result, these bones form the hypodigm of *Yarasuchus deccanensis*.

The supposed axis of *Yarasuchus deccanensis* (ISIR 334/8) is considerably longer, the centrum more dorsally arched, and the prezygapophyses more developed than in other basal archosauriforms. Therefore, this element might represent a distorted/damaged anterior postaxial cervical. As such, it is not compared with the axis of *Teleocrater rhadinus*. The anterior postaxial cervical vertebrae of *Yarasuchus deccanensis* (Extended Data Fig. 1l-m) closely resemble those of *Teleocrater rhadinus* (NMT RB505), with shared features including the presence of elongated centra with a low median ventral keel, parapophysis and diapophysis adjacent to each other, epipophysis on the postzygapophysis, and a neural spine anteroposteriorly longer than tall, with an anterior overhang, and a transversely thick, rugose distal end. In the middle and posterior cervicals, the diapophysis acquires a more posterodorsal position and is separated from the parapophysis (Extended Data Fig. 1r-s), as occurs in the middle–posterior cervicals of *Teleocrater rhadinus* (NMT RB511, RB512) and the middle cervical of *Spondylosoma absconditum* (GPIT 479/30/1).

The anterior trunk vertebrae of *Yarasuchus deccanensis* possess a low median keel on the centrum, which disappears on the middle and posterior trunk vertebrae. The trunk vertebrae possess well developed anterior and posterior centrodiapophyseal, prezygodiapophyseal, and postzygodiapophyseal laminae, as also occur in *Teleocrater rhadinus* and *Spondylosoma absconditum* (GPIT 479/30). The neural spine is relatively tall and lacks a transverse expansion in any of the trunk series (Extended Data Fig. 1q). There are no epipophyses or hypantra in the trunk vertebrae, contrasting with the presence of hyposphene-hypantrum in the trunk vertebrae of *Teleocrater rhadinus* (NMT RB516) and *Spondylosoma absconditum* (Galton 2000).

The proximal portion of a cervico-trunk rib possesses three distinct articular heads (Extended Data Fig. 1t), indicating the presence of at least one vertebra with facets for three rib heads. This condition is present in *Teleocrater rhadinus* (NHMUK PV R6795), several non-eucrocopodan basal archosauromorphs (e.g. *Prolacerta*, *Proterosuchus* spp., *Sarmatosuchus*, *Erythrosuchus*, *Cuyosuchus*; Huene 1960; Gower and Sennikov 1997; Gower 2003; Ezcurra 2016), and some pseudosuchians (e.g. *Effigia*, Nesbitt 2007; *Batrachotomus*, Gower and Schoch 2009).

The second primordial sacral of *Yarasuchus deccannensis* (Extended Data Fig. 1j) possesses morphology congruent with the equivalent elements in *Teleocrater rhadinus* (NMT RB519) and *Spondylosoma absconditum* (GPIT 479/30), including the presence of a separate posterolateral process, which is positioned dorsal and posterior to the main body of the sacral rib (see below). The neural spine is very tall, being two times taller than its respective centrum, and lacks a distal expansion (only the base of the neural spine is preserved on the second primordial sacral of *Teleocrater rhadinus*).

The scapular blade of *Yarasuchus deccanensis* is heavily crushed, but as preserved its posterior margin is considerably more concave than that of *Teleocrater rhadinus* (NMT RB480) and *Spondylosoma absconditum* (GPIT 479/30/20). The presence/absence of a sharp ridge on the posterior edge of the blade cannot be determined because of its poor preservation. The glenoid region of the scapula possesses a very subtle tuberosity above the supraglenoid lip, contrasting with *Teleocrater rhadinus* and *Spondylosoma absconditum* (GPIT 479/30/10).

The overlapping bones of the forelimbs of *Yarasuchus deccanensis* and *Teleocrater rhadinus* (i.e. humerus and ulna) are very similar to each other. The humeri

share a symmetrical proximal end in anterior view, a moderately low deltopectoral crest, a low supinator process, and a deep ectepicondylar groove (Extended Data Fig. 1n-o). The ulnae possess a very low olecranon process, a low and rounded lateral tuber (= radial ridge), and an oval end in distal view (Extended Data Fig. 1p).

The ilium of *Yarasuchus deccanensis* possesses a well-developed supraacetabular crest and a distinct concave ventral margin between the posterior and anterior ends of the ischial peduncle, as occurs in *Teleocrater rhadinus* (NHMUK PV R6795). The ischia of *Yarasuchus deccanensis* (Extended Data Fig. 1k) and *Teleocrater rhadinus* are also very similar, but that of the former species curves slightly ventrally along its distal half.

The femora and tibiae of *Yarasuchus deccanensis* (Extended Data Fig. 1c-g) and *Teleocrater rhadinus* closely resemble each other. The femur of *Yarasuchus deccanensis* is very gracile, sigmoidal in posterior view, with a very low fourth trochanter, and concave proximal and distal articular surfaces. On the anterior surface of the femur, there is a mound-like tuberosity in the same position as the anterior trochanter of riojasuchids and dinosauromorphs (Nesbitt 2011). This feature is present, with the same morphology, in several femora referred to *Yarasuchus deccanensis*. In contrast, *Teleocrater rhadinus* (NHMUK PV R6795) and *Dongusuchus efremovi* (PIN 952/15-1) possess a distinct, subtriangular scar with a proximal apex in this area, but not a mound-like structure. The tibia of *Yarasuchus deccanensis* lacks a cnemial crest and a depressed lateral posterior condyle, and the two proximal posterior condyles are approximately aligned with each other. The distal end of the tibia is subcircular to suboval with a deeply concave articular surface.

A complete left calcaneum (Extended Data Fig. 1h-i) was collected from the *Yarasuchus deccannensis* bonebed and possesses morphology very similar to that of *Teleocrater rhadinus* (NMT RB490). Therefore, this element is added to the hypodigm of the Indian species. The calcanea of both species share a subtriangular medial peg, a convex facet for articulation with the fibula, and a subquadrangular, posteriorly oriented calcaneal tuber.

No osteoderms were found in the *Teleocrater rhadinus* bonebed, suggesting that this species lacked those dermal ossifications. In contrast, several osteoderms were collected from the *Yarasuchus deccannensis* bonebed (Sen 2005). However, the osteoderms previously referred to the Indian species are larger than expected in comparison with the presacral vertebrae, and they possess very similar morphology to osteoderms associated with an erythrosuchid partial postcranium from another locality within the same formation (MDE pers. obs.). As a result, the osteoderms are tentatively excluded from the hypodigm of *Yarasuchus deccannensis* herein.

3. *Spondylosoma absconditum*

Spondylosoma absconditum (GPIT 479/30; Extended Data Fig. 1) is an archosauriform of contentious phylogenetic relationships from the late Middle−early Late Triassic (*Dinodontosaurus* Assemblage Zone) of southern Brazil (Huene 1942). *Spondylosoma* has been alternatively interpreted as a rauisuchid pseudosuchian (Galton 2000) or a possible saurischian dinosaur (Huene 1942; Langer 2004), but this taxon has not yet been included in a quantitative phylogenetic analysis. The lectotype and paralectotype were collected in Excavation 44 at the locality Baum Sanga (Chiniquá) and comprise cervical, trunk, and sacral vertebrae that were found in fairly close proximity to

partial right and left scapulae, the proximal end of a left humerus, the proximal half of a right pubis, and the distal end of a left femur (Huene 1942). In the same plate in which Huene (1942: plate 30) figured the hypodigm of *Spondylosoma absconditum*, he also figured a partial cervical vertebra and the proximal half of a left tibia that were collected from a different locality (Cynodont Sanga): there is no evidence to refer these additional elements to this species.

The two preserved cervical vertebrae of *Spondylosoma absconditum* have been damaged since the original description of Huene (1942) (Extended Data Fig. 1u-w). The most anterior of them now lacks the zygapophyses, most of the diapophyses, and the neural spine, whereas the posterior cervical has lost part of the right diapophysis and the distal end of the neural spine (Galton 2000). Based on the photographs provided by Huene (1942), the currently missing neural spine of the middle cervical was anteroposteriorly longer than tall, with an anterodorsally extending anterior margin (in lateral view), closely resembling the condition in *Teleocrater rhadinus* (NMT RB505, 511, 512) and *Yarasuchus deccanensis* (ISIR 334/9). The distal end of this neural spine was slightly transversely expanded. Epipophyses have been alternately described (Langer 2004) or reported absent (Galton 2000) in the anterior postaxial cervical vertebra of *Spondylosoma absconditum*. Because this portion of bone is not currently preserved, the presence of an epipophysis is considered uncertain and thus cannot be compared with the condition in *Teleocrater rhadinus* and *Yarasuchus deccanensis*.

The trunk vertebrae of *Spondylosoma absconditum* possess a distinct, subrectangular hyposphene (Extended Data Fig. 1z), as occurs in *Teleocrater rhadinus* (NMT RB516) and several other archosauriforms (Ezcurra 2016). The second primordial sacral rib of *Spondylosoma absconditum* has a separate posterodorsal process that is placed dorsal and posterior to the main portion of the rib (Extended Data Fig. 1aa), closely resembling the condition in *Teleocrater rhadinus*, *Yarasuchus deccanensis*, and dinosauromorphs (see below). The right scapula of *Spondylosoma absconditum* (Extended Data Fig. 1bb-cc) possesses a sharp, proximodistally-oriented ridge on the posterior margin of the scapular blade, a condition that also occurs in *Teleocrater rhadinus* and non-dinosaurian dinosauromorphs (see below).

Histological Description of *Teleocrater rhadinus*

The cross-section of a right fibula (NMT RB488) is ovoid with a long axis measuring 8 mm and a short axis measuring 7 mm (Extended Data Fig. 2a-c). A thin cortex measuring 1–1.5 mm thick surrounds the centrally located medullary cavity. Traces of the cancellous tissues and endosteal lamellae are present in the medullary cavity. Unremodelled primary woven-fibered bone composes almost the entire cortex, parallel fibered bone is present locally, and no secondary osteons are present. The vascular canals of the cortex are all primary osteons and most of these are longitudinal canals, although a few short radial canals are present. In some parts of the bone, the longitudinal canals are aligned in circumferential bands throughout the cortex. The abundance of osteocytes throughout the cortex show no preferred alignment with respect to the long axis of the bone. A break in tissue (i.e. a line of arrested growth [LAG]) is present in the outermost cortex, but no external fundamental system (EFS) is present in the outer cortex. These characters of the outer cortex indicate that the individual was

actively growing at the time of death.

The left humerus section (NMT RB476) consists of a portion of the cortex from the anterior portion of the midshaft (Extended Data Fig. 2d-f). Like the fibula, the cortex of the humerus is composed of unremodelled primary woven-fibered bone and there is no major difference between the inner cortex and the outer cortex. The vascularity is composed of longitudinal and radial canals and many of the longitudinal canals anastomose, unlike the condition of the fibula. A break in tissue is present in the outermost cortex.

The histological characters of *Teleocrater rhadinus*, including dense vascularity in both elements, high levels of anastomoses in the humerus, and osteocyte disorganization in both elements, suggest higher growth rates than those of typical stem archosaurs (Botha-Brink et al. 2011). These characters are consistent with, but not identical to, those present in the dinosaur sister group Silesauridae (*Asilisaurus kongwe*, Griffin and Nesbitt 2016; *Silesaurus opolensis*, Fostowicz-Frelik and Sulej 2010), and slower than the growth rate of the possible dinosaur or close dinosaur relative *Nyasasaurus parringtoni* (Nesbitt et al. 2013a), pterosaurs (Padian et al. 2004), and some dinosaurs (*Megapnosaurus rhodesiensis*, Chinsamy 1990). Given that we do not know the body size of the individuals of the two sampled specimens, the rate of growth cannot be directly compared to that of most early archosaurs and relatives (see Nesbitt et al. 2013a). However, we conclude that the histological characteristics are more similar to those of avian-line archosaurs than those of pseudosuchians and stem-archosaurs.

Further details of the phylogenetic analysis

1. New and revised characters added to the dataset of Nesbitt (2011) as modified by Butler et al. (2014)

Revised characters:

191. Cervical vertebrae, distal end of neural spines: (0) expansion absent; (1) laterally expanded in the middle of the anteroposterior length; (2) expanded anteriorly, so that the spine table is triangular or heart-shaped in dorsal view; (3) blade-like, but with adjacent, rounded expansions with a rugose texture.

State (3) was added to describe the neural spine morphology of *Yarasuchus deccanensis* and *Teleocrater rhadinus*.

273. Ilium, ventral margin of the acetabulum: convex where the pubic and ischial peduncles meet at an apex ventral to the acetabulum (0); concave where the pubic and ischial peduncles meet well within the ilium component of the acetabulum (1).

This character replaces the original formulation in Nesbitt (2011). As stated in Nesbitt (2011), all non-archosaurian archosauromorphs (e.g. *Erythrosuchus africanus*, NHMUK PV R3592) have character state 0 where the pubic and ischial peduncles converge ventrally to form an apex at the ventral portion of the acetabular component of the ilium. In pseudosuchians, state 0 is also prevalent and is exemplified by *Batrachotomus kupferzellensis* (SMNS 80273). In nearly all of these taxa, the lengths of the ischial and pubic peduncles are nearly the same. Taxa previously scored as having a "straight" (state 1 of Nesbitt 2011) ventral margin (e.g. *Asilisaurus kongwe*, NMT RB13) and some of the taxa (e.g. *Arizonasaurus babbitti*, MSM P4590) scored as having a

concave margin (state 2 of Nesbitt 2011) are rescored here as state (0) because even though the ischial peduncle is slightly or completely concave ventrally (see new character 414) and typically longer than the pubic peduncle, there is still a ventral apex formed between the ischial and pubic peduncles. In this newly revised character, state (1) is scored for the taxa considered to have completely open acetabula. Within Pseudosuchia, the poposauroids *Poposaurus* and shuvosaurids and the following crocodylomorphs are scored as state (1): *Dibothrosuchus* (IVPP V7907), *Kayentasuchus* (UCMP 131830), *Protosuchus richardsoni* (AMNH FR 3024), *Terrestrisuchus* (Crush 1984), *Orthosuchus* (SAM-PK-K409), and *Alligator*. Within Avemetatarsalia, all members of Dinosauria are scored as state (1), including *Saturnalia* (previously scored as state 1, straight, in Nesbitt 2011).

New characters

414. Ilium, ventral portion, ischial peduncle, lateral view: nearly straight or slightly concave (0); distinct notch (= dorsal concavity) between the posterior and anterior ends (1). (Extended Data Fig. 10)

The ischial peduncle of stem archosaurs and most archosaurs are either straight or slightly concave for the length of the peduncle (e.g. *Batrachotomus kupferzellensis*, SMNS 80273; *Erythrosuchus africanus*, NHMUK PV R3592; *Chanaresuchus bonapartei*, MCZ 4035, PVL 6244). In *Teleocrater rhadinus* (NHMUK PV R6795), *Yarasuchus deccanensis* (ISIR 334/56), and the silesaurids *Asilisaurus kongwe* (NMT RB159) and *Silesaurus opolensis* (ZPAL ABIII 404/1), there is a distinct notch about halfway between the anterior and posterior extents of the ischial peduncle. This notch is present in these forms even though the peduncle has a nearly straight ventral margin. The scoring of this character is not possible in the articulated pelvic elements of *Lagerpeton chanarensis* and is not clearly visible in any pterosaur observed for this analysis. In *Marasuchus lilloensis* (PVL 3871), the ischial peduncle seems to be straight. Ctenosauriscids, including *Arizonasaurus babbitti* (MSM 4590), and other poposauroids, such as *Qianosuchus mixtus* (IVPP V14300) and *Lotosaurus adentus* (IVPP V4880), are also scored as state 1. Taxa with largely concave margins (revised character 273 state 1) of the ventral portion of the acetabulum (e.g. *Poposaurus gracilis*, shuvosaurids, some crocodylomorphs, and dinosaurs) are scored as inapplicable for this character.

415. Fibula, posterior edge: gently rounded (0); distinct ridge paralleling the shaft (1). (Extended Data Fig. 10)

The fibula of most archosauriforms (e.g. *Chanaresuchus bonapartei*, MCZ 4035, PVL 6244) is gently rounded on the posterior edge for the length of the element. In *Teleocrater rhadinus* (NHMUK PV R6795) and the silesaurids *Asilisaurus kongwe* (NMT RB159) and *Silesaurus opolensis* (ZPAL Ab III/1930), a well-defined ridge is present on the posterior edge of the shaft for much of the length of the element. This ridge does not appear to be present in Dinosauria (*Tawa hallae*, GR 242), and cannot be scored in *Lagerpeton* and *Marasuchus* because its apparent absence might be the result of lack of preservation of such a small structure. The scar appears to be present in *Dromomeron romeri* (GR 238).

416. Primordial sacral vertebra two, sacral rib: consist of a single body in one plane (could contain a lateral notch) (0); has a separate posterolateral process positioned dorsal and posterior to the main body of the sacral rib (1). (Extended Data Fig. 10)

Primordial sacral vertebra two of most non-archosaurian eucrocopods (e.g. *Euparkeria capensis*, SAM-PK-K6049B) and archosaurs possess a sacral rib that extends posteriorly as a single body. Several non-archosauriform archosauromorphs (e.g. *Macrocnemus bassanii*, *Mesosuchus browni*, *Prolacerta broomi*) and early diverging archosauriforms (e.g. *Proterosuchus alexanderi*, NMQR 1484) have a laterally notched sacral rib, but this is not considered homologous with state 1 of this character because the sacral rib is in the same plane, just partially subdivided. In *Teleocrater rhadinus* (NMT RB519), *Yarasuchus deccanensis* (ISIR 334), *Spondylosoma absconditum* (GPIT 479/30), *Asilisaurus kongwe* (NMT RB159), and dinosaurs (e.g. *Saturnalia tupinquim*, MCP 3844-PV), posterodorsally directed processes are present dorsal and posterior of the main body of the sacral rib. These thin processes taper laterally and it is not clear if they contact the ilium in non-dinosaurian avemetatarsalians. The disjointed arrangement of the posterolaterally directed processes and the sacral rib is exaggerated in dinosaurs, essentially creating a vertically divided sacral rib. The scoring of this character is not possible in the articulated pelvic elements of *Lagerpeton* and *Marasuchus* as the processes are delicate and thin and the available specimens with exposed sacral ribs in the relevant area are damaged, roughly prepared and/or covered with matrix. This character cannot be observed in any pterosaur examined for this analysis.

417. Femur, distal end, medial condyle in posterior view: smooth surface or a small depression (0); well-defined proximodistally-oriented scar extending from the posterior portion of the condyle well proximally (1). (Extended Data Fig. 10)

The posterior (or ventral) surface of the medial condyle of the femur of non-archosaurian archosauriforms (e.g. *Erythrosuchus africanus*, NHMUK PV R3592; *Chanaresuchus bonapartei*, PVL 6244) and pseudosuchians (e.g. *Revueltosaurus callenderi*, PEFO 34561) is typically smooth or has a small scar. This scar is much broader mediolaterally and proximodistally in *Teleocrater rhadinus* (NHMUK PV R6795), *Dongusuchus efremovi* (PIN 952/15-1), *Dromomeron gregorii* (TMM 31100-1306), *Dromomeron romeri* (GR 216), *Asilisaurus kongwe* (NMT RB159), and dinosaurs (e.g. *Tawa hallae*, GR 244; *Saturnalia tupiniquim,* MCP 3944-PV). The medial edge of the scar of taxa scored as (1) is confluent with the femoral caudomedial intermuscular line (*sensu* Langer 2003). None of the *Lagerpeton* and *Marasuchus* specimens could be scored for this character because of poor preservation in this region. The pterosaur *Dimorphodon* (YPM 9182G) clearly has state 1.

418. Scapula, posterior edge of the blade just dorsal to the glenoid region: smoothly transversely convex (0); with a distinct, longitudinal sharp ridge (1).

The posterior margin of the scapula of most archosauriforms is smoothly transversely convex and featureless. In *Teleocrater rhadinus* (NHMUK PV R6795; NMT RB480) and the silesaurids *Silesaurus opolensis* (ZPAL Ab III 2534, 404-8), *Asilisaurus kongwe* (NMT RB159), and *Lewisuchus admixtus* (PULR 01), the posterior margin of the scapula bears a distinct, longitudinal sharp ridge that trends proximodistally. The ridge can sometimes be seen in lateral or medial views. The character state is currently unknown in Triassic pterosaurs, *Lagerpeton*, and *Dromomeron*. This sharp ridge is

apparently absent in *Marasuchus*, but if it was present in PVL 3871 it would have been a small, delicate feature and it is possible that it was not preserved due to taphonomic processes or over-preparation. As a result, we cannot determine the condition confidently and this character is scored for *Marasuchus* as missing data herein.

419. Cervical vertebrae, anterior and middle postaxial cervical neural spines with an anterior overhang: absent (0); present (1) (Senter 2004: 30; Ezcurra et al. 2014: 172; Pritchard et al. 2015: 115; Ezcurra 2016: 343).

The anterior margin of the neural spine slants anteriorly from its base in the anterior and middle cervicals of several non-archosauriform archosauromorphs (e.g. *Protorosaurus speneri*, BSPG 1995 I 5, cast of WMsN P47361; *Macrocnemus bassanii*, PIMUZ T4822; *Prolacerta broomi*, BP/1/2675) and some archosauriforms, including the proterochampsid *Tropidosuchus romeri* (PVL 4601), the doswelliid *Doswellia kaltenbachi* (USNM 244214), the gracilisuchids *Gracilisuchus stipanicicorum* (PULR 08) and *Turfanosuchus dabanensis* (IVPP V3237), some paracrocodylomorphs (e.g. *Qianosuchus mixtus*, *Lotosaurus adentus*, *Fasolasuchus tenax*, *Dibothrosuchus elaphros*, *Terrestrisuchus gracilis*), the sauropodomorph *Plateosaurus engelhardti* (GPIT mounted skeletons), and *Teleocrater rhadinus* (NMT RB 505), *Yarasuchus deccanensis* (ISI R334/9), and *Spondylosoma absconditum* (Huene 1942: plate 30, fig. 1; neural spine currently missing). In contrast, the anterior margin of the neural spine is vertical or slants posteriorly in lateral view in other sampled archosauromorphs.

2. Scoring changes from the dataset of Nesbitt (2011) as modified by Butler et al. (2014)

Character 144: changed from (0) to (?) in *Dimorphodon*
Character 168: changed from (0) to (1) in *Dimorphodon*
Character 195: changed from (0) to (?) in *Marasuchus*
Character 225: changed from (0) to (1) in *Chanaresuchus* and *Tropidosuchus*
Character 234: changed from (1) to (?) for the original scores of *Asilisaurus*
Character 237: changed from (0) to (1) in *Erythrosuchus africanus*
Character 265: changed from (0) to (1) in *Dimorphodon* and *Eudimorphodon*; changed from (0) to (2) in *Marasuchus*; changed from (0) to (?) in *Lagerpeton*
Character 320: changed from (1) to (0) for the original scores of *Asilisaurus*
Character 368: changed from (–) to (1) for the original scores of *Asilisaurus*
Character 371: changed from (1) to (0) for the original scores of *Asilisaurus*; changed from (1) to (0) in *Marasuchus*
Character 376: changed from (1) to (0) for the original scores of *Asilisaurus*

3. Character modified in the dataset of Ezcurra (2016)

352. Proximal tarsals, articulation between astragalus and calcaneum: roughly flat (0); concavoconvex with concavity on the calcaneum (1); concavoconvex with concavity on the astragalus (2). The fourth state of this character in Ezcurra (2016) (“fused”) was deleted and included as the independent character 606.

4. New characters added to the dataset of Ezcurra (2016) (see descriptions above)

601. Primordial sacral vertebra two, sacral rib: consists of a single body in one plane (could contain a lateral notch) (0); has a separate posterolateral process positioned dorsal and posterior to the main body of the sacral rib (1).

602. Scapula, posterior edge of the blade just dorsal to the glenoid region: smoothly transversely convex (0); with a distinct, longitudinal sharp ridge (1).

603. Ilium, ventral portion, ischial peduncle, lateral view: nearly straight or slightly concave (0); distinct notch (= dorsal concavity) between the posterior and anterior ends (1).

604. Femur, distal end, medial condyle in posterior view: smooth surface or a small depression (0); well-defined proximodistally oriented scar extending from the posterior portion of the condyle well proximally (1).

605. Fibula, posterior edge: gently rounded (0); distinct ridge paralleling the shaft (1).

606. Proximal tarsals, fusion between astragalus and calcaneum: absent (0); present (1).

5. Scoring changes from Ezcurra (2016)

After examining *Yarasuchus* in light of the anatomy of *Teleocrater*, it became clear that we could not confidently assign the maxilla attributed to *Yarasuchus* by Sen (2005). This maxilla likely belongs to an allokotosaurian archosauromorph that was found in the same bonebed as the holotype and referred specimens of *Yarasuchus* (see above). Similarly, we also question Sen's (2005) attribution of osteoderms to *Yarasuchus* (see above). Accordingly, all scorings for the maxilla and osteoderms were changed to (?).

Scorings changed from the original data matrix of Ezcurra (2016):
Characters 1, 36, 304: changed from (2) to (?) in *Yarasuchus*.
Characters 13, 52, 57, 67, 305: changed from (1) to (?) in *Yarasuchus*.
Characters 46, 53, 62, 70, 72−74, 303, 306−308: changed from (0) to (?) in *Yarasuchus*.
Character 54: changed from (0/1) to (?) in *Yarasuchus*.
Characters 58, 66, 75: changed from (1/2) to (?) in *Yarasuchus*.
Character 68: changed from (3) to (?) in *Yarasuchus*.
Character 299: changed from (4) to (?) in *Yarasuchus*.
Characters 314, 545, 546, 548, 552, 555: changed from (?) to (1) in *Yarasuchus*.
Character 359: changed from (0) to (?) in *Cuyosuchus*.
Characters 184, 401: changed from (0) to (1) in *Yarasuchus*.
Characters 430−432, 517, 518, 520−524: changed from (?) to (0) in *Dongusuchus*.
Character 433: changed from (0) to (1) in *Shansisuchus*, *Erythrosuchus*, and *Yarasuchus*.
Character 462: changed from (0) to (?) in *Yarasuchus*, *Dimorphodon*, and *Lagerpeton*, and from (0) to (2) in *Marasuchus*.
Character 466: changed from (0) to (?) in *Koilamasuchus*.
Character 484: changed from (0) to (1) in *Yarasuchus*.

Character 485: changed from (0) to (1) in *Yarasuchus*.
Character 502: changed from (0) to (1) in *Yarasuchus* and *Dongusuchus*.
Character 519: changed from (?) to (1) in *Dongusuchus*.
Character 532: changed from (3) to (-) in *Planocephalosaurus*, *Gephyrosaurus*, *Lagerpeton*, *Dimorphodon*, and *Heterodontosaurus*.
Character 536: changed from (0) to (?) in *Yarasuchus*.
Characters 543, 544, 547, 549−551, 553, 554: changed from (?) to (0) in *Yarasuchus*.
Characters 588, 589, 592, 595, 597: changed from (1) to (?) in *Yarasuchus*.
Characters 590, 591, 596: changed from (0) to (?) in *Yarasuchus*.

6. Character support for key nodes
Nesbitt (2011) dataset support
Archosauria
27 2→0 unambiguous
32 0→1 unambiguous
95 1→2
118 0→1 unambiguous
122 0→1 unambiguous
137 1→2 unambiguous
220 0→1
222 0→1 unambiguous
225 0→1 unambiguous
237 0→1 unambiguous
245 0→1 unambiguous
300 0→1
353 0→1
366 0→1 unambiguous

Avemetatarsalia
84 0→1
87 0→1
93 1→0
111 0→1
114 0→1 unambiguous
141 0→1
144 0→1 unambiguous
152 0→1
159 1→0
181 0→1 unambiguous
183 0→1 unambiguous
191 1→0
195 0→1 unambiguous
196 1→0
197 1→0
255 0→1

257 0→1
265 0→2 unambiguous
341 0→1 unambiguous
347 0→1
348 0→1
357 0→1
361 0→1
363 0→1
371 1→0
374 1→0
382 0→1
400 2→0
401 1→0
412 0→1
414 0→1
415 0→1 unambiguous
416 0→1 unambiguous
417 0→1 unambiguous
418 0→1

Aphanosauria
27 0→1
186 0→1
191 0→3
197 0→2
198 0→1
230 0→1
235 0→1
288 0→1
291 0→1
293 0→1
300 1→0
308 0→1
314 0→1
376 1→0
419 0→1 unambiguous

Ornithodira
179 0→1
218 0→1
233 0→1
234 0→1
274 0→1
299 0→1 unambiguous
301 1→0
320 0→1 unambiguous

323 0→1
345 0→1
370 0→1
373 0→1

Ezcurra (2016) dataset support
Archosauria
16 1→0
34 1→0
54 1→2 unambiguous
63 0→1
66 1→2
88 0→2
92 0→1
106 0→1
129 0→1 unambiguous
133 0→1
186 0→1
187 2→3 unambiguous
188 0→1 unambiguous
195 0→3
205 0→1
220 0→1 unambiguous
221 0→1
224 0→1
240 0→2 unambiguous
249 0→1
256 0→1
269 0→1
330 0→1
385 1→0 unambiguous
408 0→1
410 0→1
419 0→1 unambiguous
421 0→1 unambiguous
430 0→1
433 0→1
496 0→1
529 0→1 unambiguous
532 2→1 unambiguous
552 0→1 unambiguous
555 0→1 unambiguous
564 1→0
571 1→2
593 1→0 unambiguous
598 1→0

Avemetatarsalia
8 0→1
67 0→1
105 0→3
113 0→1
116 0→1
117 0→1
167 0→1
195 3→5
203 0→1
204 1→0
206 1→0
250 1→2
273 0→1
282 0→1
283 1→2
289 0→1
298 1→0
322 1→0
387 0→1 unambiguous
405 0→1
439 0→1
452 0→1
453 0→1
458 1→0
460 1→2 unambiguous
462 0→2 unambiguous
466 1→0
478 2→0
538 0→1
539 0→1
540 0→1
544 1→0 unambiguous
560 0→1
561 0→1
565 0→1
588 2→0
601 0→1 unambiguous
602 0→1
603 0→1
604 0→1 unambiguous
605 0→1

Aphanosauria
177 2→3

181 0→1
314 0→1
336 0→1
337 0→1
343 0→1 unambiguous
361 0→1
379 0→3
398 1→0
401 1→0
430 1→0
472 0→1
482 1→2
484 0→1
485 0→1
489 1→2
495 0→1
496 1→0
502 0→1

Ornithodira
1 2→0
342 0→1
352 0→1
384 1→0 unambiguous
399 0→1 unambiguous
418 0→1
427 1→2 unambiguous
457 0→1 unambiguous
464 1→0 unambiguous
466 0→2
492 0→1
508 0→1 unambiguous
532 1→3 unambiguous
545 1→0 unambiguous
546 1→2
548 1→0
553 0→2

Inclusion of *Scleromochlus taylori*

To further examine the early evolution of Avemetatarsalia, we examined the specimens of *Scleromochlus taylori*, a Late Triassic taxon previously hypothesized to be near the base of bird-line archosaurs or more closely related to pterosaurs than to other archosaurs (Huene 1914; Padian 1984; Gauthier 1986; Sereno 1991; Benton 1999). To test the relationships of *Scleromochlus taylori* among early avemetatarsalians, we scored it into the datasets of Nesbitt (2011) and Ezcurra (2016). The scores were based on direct observations made from the holotype and referred specimens, but most scores were based

on highly detailed epoxy casts provided by K. Padian and J. Gauthier to SJN. Additionally, we used previous descriptions and observations (e.g. Padian 1984; Sereno 1991; Benton 1999) of the anatomy to confirm our character scores. However, scoring *Scleromochlus taylori* remains extremely challenging given the small size and poor preservation of the moulds/casts (Benton 1999) and the fact that previous descriptions of the anatomy are at odds with each other. For example, the identifications of the ankle elements made by Sereno (1991) and Benton (1999) do not agree and this region of the anatomy is critical to the phylogenetic topology of early archosaurs (Gauthier 1986; Benton and Clark 1988; Sereno 1991; Parrish 1993; Juul 1994; Benton 1999; 2004; Brusatte et al. 2010a; Nesbitt 2011; Ezcurra, 2016). In these instances, we scored only the character states we could confirm with the casts.

We used the same methodologies and taxon sampling (with the addition of *Scleromochlus*) as those in the main phylogenetic analyses presented in the main text. Using either dataset, we recover *Scleromochlus* as an avemetatarsalian. However, the phylogenetic position differs in the two analyses. In the strict consensus of the Nesbitt (2011) dataset, we found *Scleromochlus* in a large polytomy with most aphanosaurs, *Spondylosoma*, both pterosaurs, all lagerpetids, and dinosauriforms (number of most parsimonious trees [MPTs] = 792; tree length = 1378 steps; consistency index = 0.3549; retention index = 0.7803; best score was hit 94 times of the 100 replications; Extended Data Fig. 7). The alternative positions that *Scleromochlus* adopts among the optimal trees include: as the most basal dinosauromorph (sensu Sereno et al. 2005), a lagerpetid, or a non-aphanosaurian, non-pterosaur early avemetatarsalian. In the strict consensus of the Ezcurra (2016) dataset, we found *Scleromochlus* as a dinosauromorph (sensu Sereno et al. 2005), in a polytomy with Lagerpetidae and Dinosauriformes (number of MPTs = 4; tree length = 2693 steps; consistency index = 0.2945; retention index = 0.6280; best score was hit 81 times of the 100 replications; Data Fig. S8). We reiterate that *Scleromochlus* could not be scored for many of the important characters that optimize near the base of Avemetatarsalia (e.g., femoral, ankle, and pelvic characters).

Ankle evolution in early avemetatarsalians

The ankle configurations of archosaurs and their close relatives have received extensive attention for their phylogenetic information and functional interpretations (Chatterjee 1978; 1982; Cruickshank 1979; Brinkman 1981; Cruickshank and Benton 1985; Gauthier 1986; Benton and Clark 1988; Sereno 1991; Parrish 1993; Juul 1994; Dyke 1998; Benton 1999; 2004; Brusatte et al. 2010; Nesbitt 2011; Ezcurra 2016). Most attention has focused on the origin of the extant crocodylian condition, the 'crocodile-normal' ankle configuration (movement occurs between the astragalus and the calcaneum, = mobile crurotarsal joint), through the evolution of early pseudosuchians and stem archosaurs. The evolution of the ankle in the other branch of archosaurs, Avemetatarsalia, has focused on similarities of the 'advanced mesotarsal' ankle configuration (movement occurs between the proximal tarsals and the distal tarsals) of pterosaurs (Padian 1984) and dinosauromorphs (Sereno and Arcucci 1994a, b), including dinosaurs. The mechanics of the 'crocodile-normal' ankle has been explicitly tested in extant crocodylians (Sullivan 2010, 2015) and the similarity in the ankle morphology of extant crocodylians with those of phytosaurs and suchian archosaurs highly suggests that the ankles of these forms functioned in a similar fashion (Parrish 1987). Likewise, the

‘advanced mesotarsal’ ankle is clearly present in pterosaurs (Padian 1984) and dinosauromorphs (Chatterjee 1982; Sereno 1991) and this ankle type which functioned like a hinge between the proximal and distal tarsals is present throughout Dinosauria into Aves. The differences in the morphologies between taxa with each ankle type have been clear previously; therefore, categorizing an archosaur based on its ankle type has generally been straightforward. However, a number of new key discoveries of avemetatarsalians (e.g., *Asilisaurus*, *Teleocrater*) have challenged that easy dichotomy because these new discoveries have unexpected combinations of character states present in ‘crocodile-normal’ and ‘advanced mesotarsal’ ankles. Furthermore, little evidence has been available to demonstrate character transformations between the ‘crocodile-normal’ ankle configuration, the inferred plesiomorphic condition of Archosauria, and the origin of the ‘advanced mesotarsal’ ankle configuration, although it has been previously hypothesized that the ‘advanced mesotarsal’ ankle configuration could have evolved from the ‘crocodile-normal’ ankle configuration (Chatterjee 1982).

Here we demonstrate (Extended data Fig. 5) that the key character state of the ‘crocodile-normal’ ankle configuration—a concave articulation surface of the calcaneum that fits a convex surface of the astragalus (=crurotarsal joint)—is present in *Teleocrater*, supporting the hypothesis that the ‘crocodile-normal’ ankle configuration is plesiomorphic for both Archosauria and Avemetatarsalia. Furthermore, this character state is retained in the early members of Silesauridae (*Asilisaurus* and *Lewisuchus*), the sister taxon of Dinosauria (Extended data Fig. 5). This suggests that the ‘crocodile-normal’ ankle configuration may be plesiomorphic for many of the early avemetatarsalian lineages and was independently replaced by the ‘advanced mesotarsal’ (i.e. absence of movement between the calcaneum and the astragalus) condition on more than one occasion. Alternatively, the ‘advanced mesotarsal’ condition may be a synapomorphy of Ornithodira but reversed in some silesaurids.

Several other character states have historically been associated with the ‘crocodile-normal’ ankle, such as the presence of a posteriorly projecting calcaneal tuber. Several of these character states (including the tuber) are retained in the ankle of the tiny dinosauriform *Marasuchus* (Sereno and Arcucci 1994a), although the exact articulation configuration between the astragalus and calcaneum is not known because the two elements are always preserved in articulation and the shape of the articular surfaces between the astragalus and the calcaneum cannot be seen. A clear posteriorly projecting calcaneal tuber is present in *Asilisaurus kongwe* (Extended data Fig. 5) and a reduced calcaneal tuber is also present in the early dinosaur *Herrerasaurus* (Extended data Fig. 5; Novas 1996). The size of the tuber of avemetatarsalians decreases relative to the size of the calcaneum in taxa closest to or just within Dinosauria (Extended Data Fig. 5).

To explore these observations further, we optimized the character state evolution of three key characters (see Extended Data Fig. 5) using parsimony in TNT. Optimization using the dataset of Nesbitt (2011) reconstructed a concave-convex articulation with the concavity on the calcaneum (‘crocodile-normal’) as apomorphic for Phytosauria + Archosauria and retained in Archosauria, Pseudosuchia, Avemetatarsalia, and at the base of Silesauridae. The presence of a calcaneal tuber was optimized as ancestral for Avemetatarsalia, but the ancestral condition is ambiguous for Ornithodira and nodes within non-dinosaurian dinosauromorphs. Under this phylogenetic reconstruction, it is unclear how many times the calcaneal tuber was independently lost in Ornithodira, but

because a calcaneal tuber is present in aphanosaurs and basal silesaurids, it is hypothesised to have been lost at least twice. A convex fibular facet on the calcaneum (typically associated with the 'crocodile-normal' condition) is reconstructed as plesiomorphic for Avemetatarsalia and non-dinosaurian ornithodirans. A concave fibular facet (typically associated with the 'advanced mesotarsal' condition) is optimized as independently acquired by derived silesaurids and dinosaurs (basal pterosaur condition.

The slightly different character state definitions and taxon sampling used in the Ezcurra (2016) dataset results in an ambiguous optimization for the ancestral state of the articulation between the astragalus and calcaneum in Archosauria, Avemetatarsalia, and Ornithodira. This reconstruction is not incongruent with that based upon the Nesbitt (2011) data set. As occurs with the data set of Nesbitt (2011), the presence of a calcaneal tuber is reconstructed as ancestral for Archosauria, Pseudosuchia, and Avemetatarsalia. The loss of the calcaneal tuber is optimized as apomorphic for Ornithodira, contrasting with the ambiguous reconstruction of this character in this part of the tree in the dataset of Nesbitt (2011). The fibular facet is optimized as ancestrally convex in Avemetatarsalia, but the reconstruction is ambiguous in non-dinosaurian ornithodirans, contrasting with the non-ambiguous optimization in the dataset of Nesbitt (2011).

Therefore, the typical 'crocodile-normal' ankle morphology (e.g. broad calcaneum with concave facet for reception of the astragalus and well developed calcaneal tuber) is reconstructed as ancestral for Avemetatarsalia in both datasets. The 'advanced mesotarsal' ankle configuration present in *Silesaurus* and most dinosaurs may have appeared at least twice in ornithodirans, but the optimizations of key character states are ambiguous in both datasets. As such, it is clear that the evolution of ankle character states among avemetatarsalians is more complex than traditionally reconstructed with either multiple losses of character states or multiple reacquisitions of character states that are plesiomorphic for Archosauria. Furthermore, the presence of different combinations of character states in taxa that were all once considered to have an 'advanced mesotarsal' ankle may support our observation that this ankle morphology evolved more than once in closely related taxa. The mosaic of character states present in early avemetatarsalian ankles emphasizes the reductionism of the terms 'crocodile-normal' and 'advanced mesotarsal'.

One of the remaining challenges posed by our observations is to understand when the transition from a functional 'crocodile-normal' into a functional 'advanced mesotarsal' occurs. Currently, it is not clear when the concave-convex relationship between the astragalus and calcaneum, which is clearly moveable in pseudosuchians and likely moveable in aphanosaurs, became immobile and simplified to form the 'advanced mesotarsal' ankle. Furthermore, it remains to be tested how the presence of certain character states (e.g., the convex versus concave proximal surface of the calcaneum and its interaction with the fibula) in early avemetatarsalians effect function. It is possible that the functional 'advanced mesotarsal' ankle appeared at Ornithodira and the function of the ankle of all ornithodirans is homologous even though dinosauriforms retain key character states of the 'crocodile-normal' ankle, but this has yet to be tested with anatomical models. Clearly, the evolution of early avemetatarsalian ankle morphologies and function are much more complicated than previously appreciated and need revision.

Supplementary Table S5. Occurrence data for Triassic avemetatarsalians.

Groups	Source
Aphanosauria	This paper
Pterosauria	Dalla Vecchia 2013
Lagerpetidae	Nesbitt et al. 2009; Martinez et al. 2016
Silesauridae	Nesbitt et al. 2010; Kammerer et al. 2012
Dinosauria	Langer et al. 2010; Brusatte et al. 2010b

Supplementary Table S6. Disparity estimates for major groups and time intervals (weighted mean pairwise dissimilarity [WMPD]).

	Mean WMPD	Lower confidence interval	Upper confidence interval
Total disparity per group			
Pseudosuchia	0.482	0.454	0.507
Pseudosuchia + Phytosauria	0.487	0.462	0.512
Avemetatarsalia	0.488	0.459	0.515
Pseudosuchia, time bins			
Pseudosuchia, Early–Middle Triassic	0.411	0.377	0.445
Pseudosuchia, Carnian	0.403	0.351	0.454
Pseudosuchia, early Norian	0.498	0.465	0.530
Pseudosuchia, late Norian–Rhaetian	0.454	0.415	0.492
Pseudosuchia + Phytosauria, time bins			
Pseudosuchia + Phytosauria, Early–Middle Triassic	0.413	0.380	0.446
Pseudosuchia + Phytosauria, Carnian	0.446	0.404	0.488
Pseudosuchia + Phytosauria, early Norian	0.511	0.483	0.539
Pseudosuchia + Phytosauria, late Norian–Rhaetian	0.491	0.455	0.524
Avemetatarsalia, time bins			
Avemetatarsalia, Early–Middle Triassic	0.378	0.303	0.446
Avemetatarsalia, Carnian	0.437	0.398	0.474
Avemetatarsalia, early Norian	0.487	0.437	0.533
Avemetatarsalia, late Norian–Rhaetian	0.508	0.474	0.541

Supplementary Table S7. Measurements of the hind limb elements of archosauriforms.

Taxon	Specimen	Femur (mm)	Tibia (mm)	Longest metatarsal (mm)	Source
Abrictosaurus consors	NHMUK PV RU B54	76	93	53	PMB measurements
Aetosaurus ferratus	SMNS 5770	87	65	31.5	Walker 1961
Alligator mississippiensis	TMM M-12605	158.9	125.4	75	SJN measurements
Alligator mississippiensis	TMM M-12607	140	110	65.6	SJN measurements
Alligator mississippiensis	TMM M-12606	122.7	97.2	60.3	SJN measurements
Alligator mississippiensis	TMM M-12601	120.5	97.5	60	SJN measurements
Alligator mississippiensis	TMM M-12603	89	76	50	SJN measurements
Alligator mississippiensis	TMM M-12613	62	51.9	33	SJN measurements
Alligator mississippiensis	TMM unnumbered	54	44.5	28.5	SJN measurements
Alligator mississippiensis	TMM M-12612	53	44	28	SJN measurements
Alligator mississippiensis	TMM M-12611	33.7	28.7	18.8	SJN measurements
Alligator mississippiensis	TMM M-12609	29	25.2	16.9	SJN measurements
Alligator mississippiensis	TMM M-12610	29	24.5	16.2	SJN measurements
Arcticodactylus cromptonellus	MGUH VP 3393	19.7	20.5	11.4	Jenkins et al. 2001

Asilisaurus kongwe	NMT RB159	144	124	59	SJN measurements
Campylognathoides zitteli	SMNS 50735	43	53	22	Padian 2008
Campylognathoides zitteli	UUPM R157	40	53	22	Padian 2008
Campylognathoides zitteli	MNHN HLZ 50	38	47	20	Padian 2008
Campylognathoides zitteli	CM 11424	38	47	22	Padian 2008
Carniadactylus rosenfield	MFSN 1797	37	54.2	21	Jenkins et al. 2001
Chasmatosaurus yuani	IVPP V4067	205	129	30	Young 1978
Coelophysis bauri	MNA 3318	123	136	82	Colbert 1989
Coelophysis bauri	CMNH 10971a	229	227	138	Persons and Currie 2016
Coelophysis bauri	AMNH FR 7249	196	207	110	Persons and Currie 2016
Coelophysis bauri	AMNH FR 7229	135	154	85	Persons and Currie 2016
Coelophysis bauri	AMNH FR 7246	122	136	79	Persons and Currie 2016
Coelophysis bauri	GR 148	234	242	140	Rinehart et al. 2009
Coelophysis bauri	AMNH FR 7223	209	224	126	Rinehart et al. 2009
Coelophysis bauri	AMNH FR 7224	203	221	125	Rinehart et al. 2009
Coelophysis bauri	NMMNH P-42351	181.5	217	114.6	Rinehart et al. 2009
Coelophysis bauri	CL 10971-7	165	178	105.9	Rinehart et al. 2009
Coelophysis bauri	CN 81766	150.3	170	104	Rinehart et al. 2009
Coelophysis bauri	CN 81767	144	164	97.9	Rinehart et al. 2009
Coelophysis bauri	AMNH FR 7232	140.4	154.9	86.4	Rinehart et al. 2009
Coelophysis bauri	NMMNH P-42352	135.5	159.4	95.8	Rinehart et al. 2009
Coelophysis bauri	CL 10971-4	134	153.6	94	Rinehart et al. 2009
Coelophysis bauri	NMMNH P-42200	124.6	146	80.8	Rinehart et al. 2009
Coelophysis bauri	AMNH FR 7247	123.9	136.6	85.5	Rinehart et al. 2009
Coelophysis bauri	MCZ 4334	120.9	137	81.1	Rinehart et al. 2009
Coelophysis bauri	NMMNH P-44802	119.8	141.7	79.9	Rinehart et al. 2009
Diandongosuchus fuyuanensis	ZMNH M8770	137	113	52	SJN and MRS measurements
Dimorphodon macronyx	NHMUK PV OR 41212_3	84	131	37	PMB measurements
Dorygnathus banthensis	SMNS 59293	69	95	35	Padian 2008
Dorygnathus banthensis	SMNS 50164	55	73	30	Padian 2008
Dorygnathus banthensis	MBR 1905.15	53	70	29	Padian 2008
Dorygnathus banthensis	UUPM R157	50	67	25	Padian 2008
Dorygnathus banthensis	SMNS 50914	48	74	30	Padian 2008
Dorygnathus banthensis	SMNS 52999	42	58	24	Padian 2008
Dorygnathus banthensis	BSP 1938 149	42	59	23	Padian 2008
Dorygnathus banthensis	SMNS 50702	39	50	21	Padian 2008
Eocursor parvus	SAM-PK-K8025	109	138	75	Butler et al. 2007
Eoraptor lunensis	PVSJ 512	152	156	81	Sereno et al. 2013
Eudimorphodon ranzii	MCSNB 8950	19.6	25.5	8.56	Jenkins et al. 2001
Euparkeria capensis	SAM-PK-7696	63.4	54.2	23.5	MDE measurements
Euparkeria capensis	SAM-PK-5867	55.7	47.8	7.3	MDE measurements

Gracilisuchus stipanicicorum	PVL 4597	79.9	72.4	31	Lecuona and Desojo 2011
Gracilisuchus stipanicicorum	PULR 08	59.5	46.2	24.2	MDE measurements
Herrerasaurus ischigualastensis	PVSJ 373	345	315	165	Novas 1994
Herrerasaurus ischigualastensis	PVL 2566	482	415	221	Persons and Currie 2016
Herrerasaurus ischigualastensis	PVL 2054	370	355	176	Persons and Currie 2016
Heterodontosaurus tucki	SAM-PK-K	112.2	144	67.9	Santa Luca 1980
Lagerpeton chanarensis	PVL 4619	78.8	77.2	47.2	MDE measurements
Lagerpeton chanarensis	PULR 06	77.9	92.2	49.2	MDE measurements
Liliensternus liliensterni	MB R2175	422	417	220.8	MDE measurements
Longosuchus meadei	TMM specimens	339	195	95.8	Sawin 1947
Loricata	CM 73372	275	220	85	Weinbaum 2013
Lufengosaurus huenei	IVPP V15	572	375	221	PMB measurements; Young 1941
Marasuchus lilloensis	PULR 09	41	46.6	24	Sereno and Arcucci 1994a
Marasuchus lilloensis	PVL 3871	58	68.8	38.9	MDE measurements
Marasuchus lilloensis	PVL 3870	42.2	50.1	28	Sereno and Arcucci 1994a
Megapnosaurus rhodesiensis	QG 1	208	208	132	Raath 1969
Mussaurus patagonicus	MACN-Pv SC 4111	26.9	24.9	13.1	MDE measurements
Mussaurus patagonicus	MLP 68-II-27-1	700	510	227	Otero and Pol 2013
Ornithosuchus longidens	NHMUK PV R2410	87	73	35	Walker 1964
Parringtonia gracilis	NMT RB426	74	55	23	SJN measurements
Peteinosaurus zambellii	MCSNB 3359	37	49	17.9	Jenkins et al. 2001
Poposaurus gracilis	YPM 57100	370	305	150	Gauthier et al. 2011
Postosuchus kirkpatricki	TTUP-9002	396	286	127	Weinbaum 2013
Preondactylus buffarinii	MFSN 1770	32.5	44	16	Jenkins et al. 2001
Prestosuchus chinquensis	BSP XXV 1-3/5-11/ 28-41/49	450	300	138	Krebs 1965
Proterosuchus fergusi	SAM-PK-K140	144	130	63.5	MDE measurements
Pseudochampsa ischigualastensis	PVSJ 567	140.2	124.5	53.4	Trotteyn and Ezcurra 2014
Qianosuchus mixtus	IVPP V13899	305	265	88	SJN and MRS measurements
Riojasuchus tenuisceps	PVL 3827	16.3	13.4	6	Baczko pers. com.
Saltopus elginensis	NHMUK PV R3915	55	66	38	Benton and Walker 2011
Saturnalia tupiniquim	MCP 3844-PV	152	158	84	Langer 2003
Scleromochlus taylori	NHMUK PV R3556	29	34	19	SJN measurements
Silesaurus opolensis	ZPAL Ab III/361	205	162	86	GN measurements
Stagonolepis robertsoni	various	315	187	78	Walker 1961
Stagonolepis robertsoni	various	242	144	60	Walker 1961
Syntarsus kayentakatae	MNA V2623	276	292	173	Tykoski 1998
Tawa hallae	unnumbered	176	180	79	SJN measurements
Teleocrater rhadinus	NHMUK PV R6795	170	145	74.8	SJN measurements
Terrestrisuchus gracilis	NHMUK PV R7757	57	61	22.5	PMB measurements

Ticinosuchus ferox	PIZ T2817	240	179	75	Krebs 1965
Typothorax coccinarum	NMMNH P-56299	312	147	76	Heckert et al. 2010

Supplementary Table S8. Measurements of the hind limb elements of archosauriforms used to reconstruct the length of metatarsal 3 of *Teleocrater rhadinus*. Sources of the data are found in Supplementary Table S7.

Taxon	Specimen	Femur (mm)	Tibia (mm)	Metatarsal 3 (mm)	Proximal width max (mm)
Abrictosaurus consors	NHMUK PV RU B54	76	93	53	8
Alligator mississippiensis	TMM M-12609	29	25.2	16.9	3.2
Alligator mississippiensis	TMM M-12611	33.7	28.7	18.8	4
Alligator mississippiensis	TMM M-12612	53	44	28	5.8
Alligator mississippiensis	TMM unnumbered	54	44.5	28.5	5.9
Alligator mississippiensis	TMM M-12613	62	51.9	33	6.9
Alligator mississippiensis	TMM M-12603	89	76	50	9.3
Alligator mississippiensis	TMM M-12606	122.7	97.2	60.3	13.5
Alligator mississippiensis	TMM M-12601	120.5	97.5	60	14.2
Alligator mississippiensis	TMM M-12607	140	110	65.6	16.6
Alligator mississippiensis	TMM M-12605	158.9	125.4	75	18
Asilisaurus kongwe	NMT RB159	144	124	59	16
Eocursor parvus	SAM-PK-K8025	109	138	75	7
Euparkeria capensis	SAM-PK-K7696	63.4	54.2	22.5	3.7
Gracilisuchus stipanicicorum	PULR 08	59.5	46.2	24.2	1.8
Heterodontosaurus tucki	SAM-PK-K	112.2	144	67.9	5.9
Lagerpeton chanarensis	PULR 06	77.9	92.2	43.3	4.6
Lagerpeton chanarensis	PVL 4619	78.8	77.2	43.3	4.7
Longosuchus meadei	TMM specimens	339	195	95.8	80.3
Lufengosaurus huenei	IVPP V15	572	375	221	67
Marasuchus lilloensis	PVL 3871	58	68.8	38.9	2.7
Megapnosaurus rhodesiensis	QG 1	208	208	132	20
Mussaurus patagonicus	MACN-Pv SC 4111	26.9	24.9	13.1	3
Mussaurus patagonicus	MLP 68-II-27-1	700	510	227	65
Parringtonia gracilis	NMT RB426	74	55	23	8
Proterosuchus fergusi	SAM-PK-K140	144	130	57	9.7
Saturnalia tupiniquim	MCP 3844-PV	152	158	84	20
Syntarsus kayentakatae	MNA V2623	276	292	173	14.6
Tawa hallae	GR unnumbered	176	180	79	13
Teleocrater rhadinus	NHMUK PV R6795	170	145		17
Ticinosuchus ferox	PIMUZ T2817	240	179	75	25

Institutional Abbreviations. AMNH, American Museum of Natural History, New York, New York, U.S.A.; BSP, Bayerische Staatssammlung für Paläontologie und Geologie, München, Germany; CM, Carnegie Museum of Natural History, Pittsburg, Pennsylvania, U.S.A.; CMNH, Cleveland Museum of Natural History, Cleveland, Ohio, U.S.A.; GPIT, Paläontologische Sammlung der Universität Tübingen, Tübingen, Germany; GR, Ruth Hall Museum of Paleontology at Ghost Ranch, New Mexico, U.S.A.; ISI, Indian Statistical Institute, Kolkata, India; IVPP, Institute of Vertebrate Paleontology and Paleoanthropology, Beijing, China; MACN-Pv, Museo Argentino de Ciencias Naturales "Bernardino Rivadavia", Paleontología de Vertebrados, Buenos Aires, Argentina; MB, Museum für Naturkunde, Berlin, Germany; MCSNB, Museo Civico di Scienze Naturali di Bergamo, Italy; MCP, Museu de Ciências e Tecnologia da Pontifícia Universidade Católica do Rio Grande do Sul, Porto Alegre, Brazil; MCZ, Museum of Comparative Zoology, Harvard University, Cambridge, Massachusetts, U.S.A.; MFSN, Museo Friulano di Storia Naturale, Udine, Italy; MGUH, Geological Museum, University of Copenhagen, Denmark; MLP, Museo de La Plata, La Plata, Argentina; MNA, Museum of Northern Arizona, Flagstaff, Arizona, U.S.A.; MNHN, Muséum national d'Histoire naturelle, Paris, France; MSM, Arizona Museum of Natural History, Mesa, Arizona, U.S.A.; NHMUK, Natural History Museum, London, U.K.; NMMNH, New Mexico Museum of Natural History and Science, Albuquerque, New Mexico, U.S.A.; NMQR, National Museum, Bloemfontein, South Africa; NMT, National Museum of Tanzania, Dar es Salaam, Tanzania; PEFO, Petrified Forest National Park, Arizona, U.S.A.; PIMUZ, Paläontologisches Institut und Museum der Universität Zürich, Zürich, Switzerland; PIN, Paleontological Institute of the Russian Academy of Sciences, Moscow, Russia; PULR, Paleontología, Universidad Nacional de La Rioja, La Rioja, Argentina; PVL, Paleontología de Vertebrados, Instituto Miguel Lillo, Tucumán, Argentina; PVSJ, División de Paleontología de Vertebrados del Museo de Ciencias Naturales y Universidad Nacional de San Juan, San Juan, Argentina; SAM-PK, Iziko South African Museum, Cape Town, South Africa; SMNS, Staatliches Museum für Naturkunde, Stuttgart, Germany; TMM, Jackson School of Geosciences Vertebrate Paleontology Laboratory, University of Texas at Austin, Austin, Texas, U.S.A.; TTUP, Texas Tech University Museum, Lubbock, Texas, U.S.A.; UCMP, University of California Museum of Paleontology, Berkeley, California, U.S.A.; UMZC, University Museum of Zoology, Cambridge, U.K.; USNM, National Museum of Natural History Smithsonian Institution, Washington, D.C., U.S.A.; UUPM, Palaeontological Museum, University of Uppsala, Sweden; WMsN, Westfälisches Museum für Naturkunde, Münster, Germany; YPM, Yale Peabody Museum, New Haven, Connecticut, U.S.A.; ZMNH, Zhejiang Museum of Natural History, Hangzhou, China; ZPAL, Institute of Paleobiology of the Polish Academy of Sciences, Warsaw, Poland.

References

1 Benton, M. J. *Scleromochlus taylori* and the origin of dinosaurs and pterosaurs. *Philosophical Transactions of the Royal Society of London, Series B* **354**, 1423–1446 (1999).

2 Benton, M. J. in *The Dinosauria, 2nd Edition* (eds David B. Weishampel, Peter Dodson, & Halszka Osmolska) 7–19 (University of California Press, 2004).

3 Benton, M. J. & Clark, J. M. in *The Phylogeny and Classification of the Tetrapods, Volume 1: Amphibians, Reptiles, Birds Systematics Association Special Volume 35A* (ed M. J. Benton) 295–338 (Clarendon Press, 1988).
4 Botha-Brink, J. & Smith, R. M. Osteohistology of the Triassic archosauromorphs *Prolacerta*, *Proterosuchus*, *Euparkeria*, and *Erythrosuchus* from the Karoo Basin of South Africa. *Journal of Vertebrate Paleontology* **31**, 1238–1254 (2011).
5 Brinkman, D. The origin of the crocodiloid tarsi and the interrelationships of thecodontian archosaurs. *Breviora* **464**, 1–23 (1981).
6 Brusatte, S. L., Benton, M. J., Desojo, J. B. & Langer, M. C. The higher-level phylogeny of Archosauria (Tetrapoda: Diapsida). *Journal of Systematic Palaeontology* **8**, 3–47 (2010a).
7 Brusatte, S. L., Benton, M. J., Ruta, M. & Lloyd, G. T. Superiority, competition, and opportunism in the evolutionary radiation of dinosaurs. *Science* **321**, 1485–1488 (2008).
8 Brusatte, S. L. *et al.* The origin and early radiation of dinosaurs. *Earth-Science Reviews* **101**, 68–100 (2010b).
9 Butler, R. J., Barrett, P. M., Abel, R. L. & Gower, D. J. A possible ctenosauriscid archosaur from the Middle Triassic Manda Beds of Tanzania. *Journal of Vertebrate Paleontology* **29**, 1022–1031 (2009).
10 Butler, R. J., Smith, R. M. H. & Norman, D. B. A primitive ornithischian dinosaur from the Late Triassic of South Africa and the early evolution and diversification of Ornithischia. *Proceedings of the Royal Society of London, Biological Sciences* **274**, 2041–2046 (2007).
11 Butler, R. J. *et al.* New clade of enigmatic early archosaurs yields insights into early pseudosuchian phylogeny and the biogeography of the archosaur radiation. *BMC Evolutionary Biology* **14**, 128 (2014).
12 Charig, A. J. *New Triassic archosaurs from Tanganyika including Mandasuchus and Teleocrater* PhD thesis, University of Cambridge, (1956).
13 Chatterjee, S. A primitive parasuchid (Phytosaur) reptile from the Upper Triassic Maleri Formation of India. *Palaentology* **21**, 83–127 (1978).
14 Chatterjee, S. Phylogeny and classification of thecodontian reptiles. *Nature* **295**, 317–320 (1982).
15 Chinsamy, A. Physiological implications of the bone histology of *Syntarsus rhodesiensis* (Saurischia: Theropoda). *Palaeontologia Africana* **27**, 77–82 (1990).
16 Colbert, E. H. The Triassic dinosaur *Coelophysis*. *Museum of Northern Arizona Bulletin* **57**, 1–160 (1989).
17 Cope, E. D. Synopsis of the extinct Batrachia, Reptilia, and Aves of North America. *Transactions of the American Philosophical Society* **40**, 1–252 (1869).
18 Cox, C. B. The Pangaea dicynodont *Rechnisaurus* and the comparative biostratigraphy of Triassic dicynodont faunas. *Palaeontology* **34**, 767–784 (1991).
19 Cox, C. B. & Li, J.-L. A new genus of Triassic dicynodont from East Africa and its classification. *Palaeontology* **26**, 389–406 (1983).
20 Crompton, A. W. On some Triassic cynodonts from Tanganyika. *Proceedings of the Zoological Society of London* **1125**, 617–669 (1955).
21 Cruickshank, A. Ankle joint in some early archosaurs. *South African Journal of Science* **75**, 168–178 (1979).

22 Cruickshank, A. Biostratigraphy and classification of a new Triassic dicynodont from East Africa. *Modern Geology* **10**, 121–131 (1986).
23 Cruickshank, A. & Benton, M. Archosaur ankles and the relationships of the thecodontian and dinosaurian reptiles. *Nature* **317**, 715–717 (1985).
24 Dalla Vecchia, F. M. in *Anatomy, Phylogeny, and Palaeobiology of Early Archosaurs and their Kin* Vol. 379 (eds S.J. Nesbitt, J.B. Desojo, & R.B. Irmis) 119–155 (Geological Society, London, Special Volume, 2013).
25 Díaz-Molina, M. Geometry and lateral accretion patterns in meander loops. Examples from the Upper Oligocene-Lower Miocene, Loranca Basin, Spain. *Special Publication of the International Association of Sedimentologists* **17**, 115–132 (1993).
26 Dyke, G. J. Does archosaur phylogeny hinge on the ankle joint? *Journal of Vertebrate Paleontology* **18**, 558–562 (1998).
27 Ezcurra, M. D. The phylogenetic relationships of basal archosauromorphs, with an emphasis on the systematics of proterosuchian archosauriforms. *PeerJ* **4**, e1778; DOI 1710.7717/peerj.1778 (2016).
28 Ezcurra, M. D., Scheyer, T. M. & Butler, R. J. The origin and early evolution of Sauria: reassessing the Permian saurian fossil record and the timing of the crocodile-lizard divergence. *PloS one* **9**, e89165 (2014).
29 Fostowicz-Frelik, Ł. & Sulej, T. Bone histology of *Silesaurus opolensis* Dzik, 2003 from the Late Triassic of Poland. *Lethaia* **43**, 137–148 (2010).
30 Galton, P. M. Are *Spondylosoma* and *Staurikosaurus* (Santa Maria Formation, Middle-Upper Triassic, Brazil) the oldest saurischian dinosaurs? *Paläontologische Zeitschrift* **74**, 393–423 (2000).
31 Gauthier, J. Saurischian monophyly and the origin of birds. *Memoirs of the California Academy of Sciences* **8**, 1–55 (1986).
32 Gauthier, J. & Padian, K. in *The Beginning of Birds* (eds M.K. Hecht, J.H. Ostrom, G. Viohl, & P. Wellnhofer) 185–197 (Freunde des Jura Museums, 1985).
33 Gauthier, J. A., Nesbitt, S. J., Schachner, E., Bever, G. S. & Joyce, W. G. The bipedal stem crocodilian *Poposaurus gracilis*: inferring function in fossils and innovation in archosaur locomotion. *Bulletin of the Peabody Museum of Natural History* **52**, 107–126 (2011).
34 Gower, D. J. Osteology of the early archosaurian reptile *Erythrosuchus africanus* Broom. *Annals of the South African Museum* **110**, 1–84 (2003).
35 Gower, D. J. & Schoch, R. R. Postcranial anatomy of the rauisuchian archosaur *Batrachotomus kupferzellensis*. *Journal of Vertebrate Paleontology* **29**, 103–122 (2009).
36 Gower, D. J. & Sennikov, A. G. *Sarmatosuchus* and the early history of the Archosauria. *Journal of Vertebrate Paleontology* **17**, 60–73 (1997).
37 Griffin, C. T. & Nesbitt, S. J. The femoral ontogeny and long bone histology of the Middle Triassic (?late Anisian) dinosauriform *Asilisaurus kongwe* and implications for the growth of early dinosaurs. *Journal of Vertebrate Paleontology*, e1111224, doi:10.1080/02724634.2016.1111224 (2016).
38 Heckert, A. B. *et al.* Articulated skeletons of the aetosaur *Typothorax coccinarum* Cope (Archosauria: Stagonoleopididae) from the Upper Triassic Bull Canyon

Formation (Revueltian: early-mid Norian), eastern New Mexico, USA. *Journal of Vertebrate Paleontology* **30**, 619–642 (2010).
39 Hopson, J. A. in *Early Evolutionary History of the Synapsida* (eds C.F. Kammerer, K.D. Angielczyk, & J. Fröbisch) 233–253 (Springer Science, 2014).
40 Howie, A. A. A new capitosaurid labyrinthodont from East Africa. *Palaeontology* **13**, 210–253 (1970).
41 Huene, F. v. Beitrage zur Geschichte der Archisaurier. *Geologishe und Paläontologische Abhandlungen* **13**, 1–53 (1914).
42 Huene, F. v. Ein grosser Stagonolepide aus der jüngeren Trias Ostafrikas. *Neues Jahrbuch für Geologie und Paläeontologie, Beilage-Bände Abt. B* **80**, 264–278 (1938).
43 Huene, F. v. Ein kleiner Pseudosuchier und ein Saurischier aus den ostafrikanischen Mandaschichten. *Neues Jahrbuch für Geologie und Paläeontologie, Beilage-Bände Abt. B* **81**, 61–69 (1939).
44 Huene, F. v. Die Anomodontier des Ruhuhu-Gebeites in der Tübinger Sammlung. *Palaeontographica* **94**, 155–184 (1942).
45 Huene, F. v. *Die fossilen Reptilien des Südamerikanischen Gondwanalandes*. (C.H. Beck, 1942).
46 Huene, F. v. Ein grosser pseudosuchier aus der Orenburger Trias. *Palaeontographica Abteilung A* **114**, 105–111 (1960).
47 Jenkins Jr, F. A., Shubin, N. H., Gatesy, S. M. & Padian, K. A diminutive pterosaur (Pterosauria: Eudimorphodontidae) from the Greenlandic Triassic. *Bulletin of the Museum of Comparative Zoology* **156**, 151–170 (2001).
48 Juul, L. The phylogeny of basal archosaurs. *Palaeontologia Africana* **31**, 1–38 (1994).
49 Kammerer, C. F., Nesbitt, S. J. & Shubin, N. H. The first basal dinosauriform (Silesauridae) from the Late Triassic of Morocco. *Acta Palaeontologica Polonica* **57**, 277–284, doi:10.4202/app.2011.0015 (2012).
50 Krebs, B. Die Triasfauna der Tessiner Kalkalpen. XIX. *Ticinosuchus ferox*, nov. gen. nov. sp. Ein neuer Pseudosuchier aus der Trias des Monte San Georgio. *Schweizersiche Palaontologische, Abhandlungen* **81**, 1–140 (1965).
51 Langer, M. C. The pelvic and hind limb anatomy of the stem-sauropodomorph *Saturnalia tupiniquim* (Late Triassic, Brazil). *PaleoBios* **23**, 1–40 (2003).
52 Langer, M. C. in *The Dinosauria, 2nd Edition* (eds David B. Weishampel, Peter Dodson, & Halszka Osmólska) 25–46 (University of California Press, 2004).
53 Langer, M. C., Ezcurra, M. D., Bittencourt, J. S. & Novas, F. E. The origin and early evolution of dinosaurs. *Biological Reviews* **85**, 55–110 (2010).
54 Larkin, N. *Description of a new Triassic dicynodont from the Manda Formation of Tanzania* M.Sc. thesis, University College (1994).
55 Lautenschlager, S. & Desojo, J. B. Reassessment of the Middle Triassic rauisuchian archosaurs *Ticinosuchus ferox* and *Stagonosuchus nyassicus*. *Paläontologische Zeitschrift* **85**, 357–381 (2011).
56 Lecuona, A. & Desojo, J. Hind limb osteology of *Gracilisuchus stipanicicorum* (Archosauria: Pseudosuchia). *Earth and Environmental Science Transactions of the Royal Society of Edinburgh* **102**, 105–128 (2011).

57 Martínez, R. N., Apaldetti, C., Correa, G. A. & Abelín, D. A Norian lagerpetid dinosauromorph from the Quebrada Del Barro Formation, northwestern Argentina. *Ameghiniana* **53**, 1–13 (2016).
58 Nesbitt, S. J. The anatomy of *Effigia okeeffeae* (Archosauria, Suchia), theropod convergence, and the distribution of related taxa. *Bulletin of the American Museum of Natural History* **302**, 1–84 (2007).
59 Nesbitt, S. J. The early evolution of archosaurs: relationships and the origin of major clades. *Bulletin of the American Museum of Natural History* **352**, 1–292 (2011).
60 Nesbitt, S. J., Barrett, P. M., Werning, S., Sidor, C. A. & Charig, A. The oldest dinosaur? A Middle Triassic dinosauriform from Tanzania. *Biology Letters* **9**, 20120949, doi:10.1098/rsbl.2012.0949 (2013a).
61 Nesbitt, S. J., Butler, R. J. & Gower, D. J. A new archosauriform (Reptilia: Diapsida) from the Manda beds (Middle Triassic) of southwestern Tanzania. *PLoS One*, 8(9): e72753. doi:72710.71371/journal.pone.0072753 (2013b).
62 Nesbitt, S. J. *et al.* Hindlimb osteology and distribution of basal dinosauromorphs from the Late Triassic of North America. *Journal of Vertebrate Paleontology* **29**, 498–516 (2009).
63 Nesbitt, S. J., Sidor, C. A., Angielczyk, K. D., Smith, R. M. H. & Tsuji, L. A. A new archosaur from the Manda beds (Anisian: Middle Triassic) of southern Tanzania and its implications for character optimizations at Archosauria and Pseudosuchia. *Journal of Vertebrate Paleontology* **34**, 1357–1382 (2014).
64 Nesbitt, S. J. *et al.* Ecologically distinct dinosaurian sister group shows early diversification of Ornithodira. *Nature* **464**, 95–98 (2010).
65 Novas, F. E. New information on the systematics and postcranial skeleton of *Herrerasaurus ischigualastensis* (Theropoda: Herrerasauridae) from the Ischigualasto Formation (Upper Triassic) of Argentina. *Journal of Vertebrate Paleontology* **13**, 400–423 (1994).
66 Otero, A. & Pol, D. Postcranial anatomy and phylogenetic relationships of *Mussaurus patagonicus* (Dinosauria, Sauropodomorpha). *Journal of Vertebrate Paleontology* **33**, 1138–1168 (2013).
67 Padian, K. in *Third Symposium on Mesozoic Terrestrial Ecosystems, Short Papers* (eds W.E. Reif & F. Westphal) 163–168 (Attempto Verlag, Tubingen University Press, 1984).
68 Padian, K. The Early Jurassic pterosaur *Dorygnathus banthensis* (Theodori, 1830) and the Early Jurassic pterosaur *Campylognathoides* Strand, 1928. *Special Papers in Palaeontology* **80**, 1–107 (2008).
69 Padian, K., Horner, J. R. & de Ricqlès, A. Growth in small dinosaurs and pterosaurs: the evolution of archosaurian growth strategies. *Journal of Vertebrate Paleontology* **24**, 555–571 (2004).
70 Parrish, J. M. The origin of crocodilian locomotion. *Paleobiology* **13**, 396–414 (1987).
71 Parrish, J. M. Phylogeny of the Crocodylotarsi, with reference to archosaurian and crurotarsan monophyly. *Journal of Vertebrate Paleontology* **13**, 287–308 (1993).

72 Persons IV, W. S. & Currie, P. J. An approach to scoring cursorial limb proportions in carnivorous dinosaurs and an attempt to account for allometry. *Scientific reports* **6** (2016).
73 Pritchard, A. C., Turner, A. H., Nesbitt, S. J., Irmis, R. B. & Smith, N. D. Late Triassic tanystropheid (Reptilia, Archosauromorpha) remains from northern New Mexico (Petrified Forest Member, Chinle Formation): insights into distribution, morphology, and paleoecology of Tanystropheidae. *Journal of Vertebrate Paleontology*, 10.1080/02724634.02722014.02911186 (2015).
74 Raath, M. A. A new coelurosaurian dinosaur from the Forest Sandstone of Rhodesia. *Arnoldia* **28**, 1–25 (1969).
75 Rinehart, L. F., Lucas, S. G., Heckert, A. B., Spielmann, J. A. & Celeskey, M. D. *The Paleobiology of Coelophysis bauri (Cope) from the Upper Triassic (Apachean) Whitaker quarry, New Mexico, with detailed analysis of a single quarry block.* Bulletin 45 (New Mexico Museum of Natural History and Science, 2009).
76 Santa Luca, A. P. The postcranial skeleton of *Heterodontosaurus tucki* (Reptilia, Ornithischia) from the Stormberg of South Africa. *Annals of the South African Museum* **79**, 159–211 (1980).
77 Sawin, H. J. The pseudosuchian reptile *Typothorax meadei*. *Journal of Paleontology* **21**, 201–238 (1947).
78 Sen, K. A new rauisuchian archosaur from the Middle Triassic of India. *Palaeontology* **48**, 185–196 (2005).
79 Senter, P. Phylogeny of Drepanosauridae (Reptilia: Diapsida). *Journal of Systematic Palaeontology* **2**, 257-268 (2004).
80 Senter, P. Phylogenetic taxonomy and the names of the major archosaurian (Reptilia) clades. *Paleobios* **25**, 1–7 (2005).
81 Sereno, P. C. Basal archosaurs: phylogenetic relationships and functional implications. *Society of Vertebrate Paleontology Memoir* **2**, 1–53 (1991).
82 Sereno, P. C. & Arcucci, A. B. Dinosaurian precursors from the Middle Triassic of Argentina: *Marasuchus lilloensis*, gen. nov. *Journal of Vertebrate Paleontology* **14**, 53–73 (1994a).
83 Sereno, P. C. & Arcucci, A. B. Dinosaurian precursors from the Middle Triassic of Argentina: *Lagerpeton chanarensis*. *Journal of Vertebrate Paleontology* **13**, 385–399 (1994b).
84 Sereno, P. C., Martínez, R. N. & Alcober, O. A. Osteology of Eoraptor lunensis (Dinosauria, Sauropodomorpha). *Journal of Vertebrate Paleontology* **32**, 83–179 (2013 (for 2012)).
85 Sereno, P. C., McAllister, S. & Brusatte, S. L. TaxonSearch: a relational database for suprageneric taxa and phylogenetic definitions. *PhyloInformatics* **8**, 1–21 (2005).
86 Smith, N. D., Cross, T. A., Dufficy, J. P. & Clough, S. R. Anatomy of an avulsion. *Sedimentology* **36**, 1–23 (1989).
87 Smith, R. M. H. Sedimentology and ichnology of floodplain palaeosurfaces in the Beaufort Group (Late Permian), Karoo Sequence, South Africa. *Palaios* **8**, 339–357 (1993).

88 Stockley, G. M. The geology of the Ruhuhu coalfields, Tanganyika Territory. *Quarterly Journal of the Geological Society of London* **88**, 610–622 (1932).
89 Sullivan, C. The role of the calcaneal 'heel'as a propulsive lever in basal archosaurs and extant monitor lizards. *Journal of Vertebrate Paleontology* **30**, 1422–1432 (2010).
90 Sullivan, C. in *Great Transformations in Vertebrate Evolution* (eds K.P. Dial, N. Shubin, & E.L. Brainerd) 107–124 (Chicago University Press, 2015).
91 Trotteyn, M. J. & Ezcurra, M. D. Osteology of *Pseudochampsa ischigualastensis* gen. et comb. nov.(Archosauriformes: Proterochampsidae) from the early Late Triassic Ischigualasto Formation of northwestern Argentina. *PloS one* **9**, e111388 (2014).
92 Tsuji, L., Sidor, C., Smith, R. & Angielczyk, K. The first procolophonid from the Manda Beds of southern Tanzania and its implications for Middle Triassic biogeography. *Journal of Vertebrate Paleontology, Program and Abstracts* **2013** (2013a).
93 Tsuji, L. A., Sobral, G. & Müller, J. *Ruhuhuaria reiszi*, a new procolophonoid reptile from the Triassic Ruhuhu Basin of Tanzania. *Comptes Rendus Palevol* **12**, 487-494 (2013b).
94 Tykoski, R. *The osteology of Syntarsus kayentakatae and its implications for ceratosaurid phylogeny* Master's thesis, The University of Texas at Austin, (1998).
95 Walker, A. D. Triassic reptiles from the Elgin area: *Stagonolepis*, *Dasygnathus* and their allies. *Philosophical Transactions of the Royal Society of London, Series B* **244**, 103–204 (1961).
96 Walker, A. D. Triassic reptiles from the Elgin area: *Ornithosuchus* and the origin of carnosaurs. *Philosophical Transactions of the Royal Society of London, Series B* **248**, 53–134 (1964).
97 Weinbaum, J. C. in *Anatomy, Phylogeny and Palaeobiology of Early Archosaurs and their Kin* (eds S. J. Nesbitt, J. B. Desojo, & R. B. Irmis) 525–553 (The Geological Society of London, 2013).
98 Wynd, B. M. *et al.* First occurrence of *Cynognathus* in Tanzania and Zambia, with biostratigraphic implications for the age of Triassic strata in southern Pangea. *Journal of Vertebrate Paleontology, Program and Abstracts, 2016* **36**, 254 (2016).
99 Young, C. A complete osteology of *Lufengosaurus huenei* Young (gen. et sp. nov.). *Palaeontologia Sinica, Series C* **7**, 1–53 (1941).
100 Young, C. A complete skeleton of *Chasmatosaurus yuan*i from Xinjinang. *Memoirs of the Institute of Vertebrate Paleontology and Paleoanthropology, Academia Sinica, Series B* **13**, 26–46 (1978).